



**QUEEN'S
UNIVERSITY
BELFAST**

SCHOOL OF
MECHANICAL
AND AEROSPACE
ENGINEERING

Final Project Report

MEE 7012

Low-velocity impact analysis of auxetic cored structures

| | |
|-----------|--|
| Author | Aayush Sharma [40242138] |
| Programme | MSc Mechanical Engineering with Management |
| Date | 30 August 2019 |

Project Description

Sandwich composite structures are an efficient solution to achieving high specific strength and stiffness. However, these structures are susceptible to in-service low velocity impact damage (e.g. hail stones, tool drop, and runaway debris) which may have a significant detrimental influence on their integrity. As a consequence, in aviation industry, certification authorities require that susceptible aircraft components must be tested to prove their capability to withstand low-velocity impact without suffering critical damage. Sandwich structures are often formed from two face sheets and a core. Different approaches towards the development of more efficient core materials have led to an interest in auxetic structures. Auxetic refers to a negative Poisson's ratio which is a meta-material property and there is evidence in the literature that they are highly effective under impact loading. Thus, understanding the behaviour of auxetic cored sandwich structures subjected to low velocity impact is very important to design more reliable structures.

Summary

Auxetic Structures are components possessing a negative Poisson's ratio that showcase high stiffness to weight ratio. The project covers the comparative study between Auxetic and Non Auxetic structures when subjected to low velocity impact. Three types of configurations were selected for the study; re-entrant, double arrowhead and honeycomb structures. Two different materials with varying mechanical properties were chosen to produce the specimen to check the effect of different mechanical characteristics on the test results; Nylon – soft, flexible and Onyx – hard, stiff. The samples were designed using CAD, which was used as blueprint to 3D print the designed samples using the Markforged Mark Two printers. The low velocity impact test was carried out as per ASTM d3763 standard. The experimental results showed that the nylon samples provided better resistance on comparison with onyx samples, as onyx was found to be more brittle. Nylon double arrowhead specimen showcased minimum indentation impact, onyx re-entrant specimen absorbed maximum energy and nylon honeycomb specimen was the most ductile of all the specimen.

Acknowledgments

The author would like to thank Dr Zafer Kazanci for providing continuous support, guidance and supervision throughout the project period. The author is grateful to Dr Zahur Ullah for provide guidance in the absence of Dr Kazanci.

The author would also like to thank Dr Bronagh Millar, PhD students; Clare Burnett and Farzaneh Hassani in helping out during the impact test experiment and 3D printing of specimens.

Contents

| | |
|---|------|
| Project Description..... | i |
| Summary | ii |
| Acknowledgments..... | iii |
| List of Tables | vi |
| List of Figures | vi |
| List of Equations..... | vii |
| Work Package | viii |
| Nomenclature | ix |
| 1.0 Introduction | 10 |
| 2.0 Literature Review | 12 |
| 2.1 Cellular Materials | 12 |
| 2.1.1 Re-entrant Structures | 13 |
| 2.1.2 Double Arrowhead Structures | 14 |
| 2.1.3 Polygon Rotating Models | 14 |
| 2.1.4 Chiral Models | 15 |
| 2.1.5 Crumpled sheet models | 16 |
| 2.2 Auxetic Material Properties | 17 |
| 2.2.1 Indentation Resistance | 17 |
| 2.2.2 Synclasticity..... | 18 |
| 2.2.3 Variable permeability..... | 19 |
| 2.2.4 Energy absorption | 19 |
| 2.3 Auxetic Structure Applications..... | 20 |
| 2.3.1 Protective Devices..... | 20 |
| 2.3.2 Auxetic Nails..... | 20 |
| 2.3.3 Smart Piezoelectric Sensors | 20 |
| 2.3.4 Textile..... | 21 |
| 2.4 Auxetic Core Fabrication | 21 |

| | |
|---|----|
| 3.0 Project Objectives | 22 |
| 4.0 Experimental Procedure | 22 |
| 4.1 Unit Cell Design | 22 |
| 4.2 Sample Design | 24 |
| 4.3 Sample Production | 25 |
| 4.4 Drop-weight impact Testing..... | 27 |
| 5.0 Results and Discussions | 29 |
| 5.1 Experimental Results and Plots..... | 29 |
| 5.2 Crashworthiness Performance Indicators..... | 33 |
| 5.3 Manufacturing Defects and Discrepancies | 34 |
| 5.3.1 Mass Defect | 34 |
| 5.3.2 Printing Errors | 35 |
| 6.0 Conclusions | 36 |
| 6.1 Future Scope | 36 |
| References | 37 |
| Appendix A Project management | 42 |

List of Tables

| | |
|---|----|
| Table 1 Design Parameters | 23 |
| Table 2 Design Parameters of Unit Cell | 24 |
| Table 3 Print Settings of Markforged Mark 2 | 25 |
| Table 4 Material Properties | 25 |
| Table 5 Equipment and Test Parameters..... | 28 |
| Table 6 Experimental Results for 50.78J Impact Energy..... | 29 |
| Table 7 Discrepancy in the theoretical and actual weight..... | 34 |

List of Figures

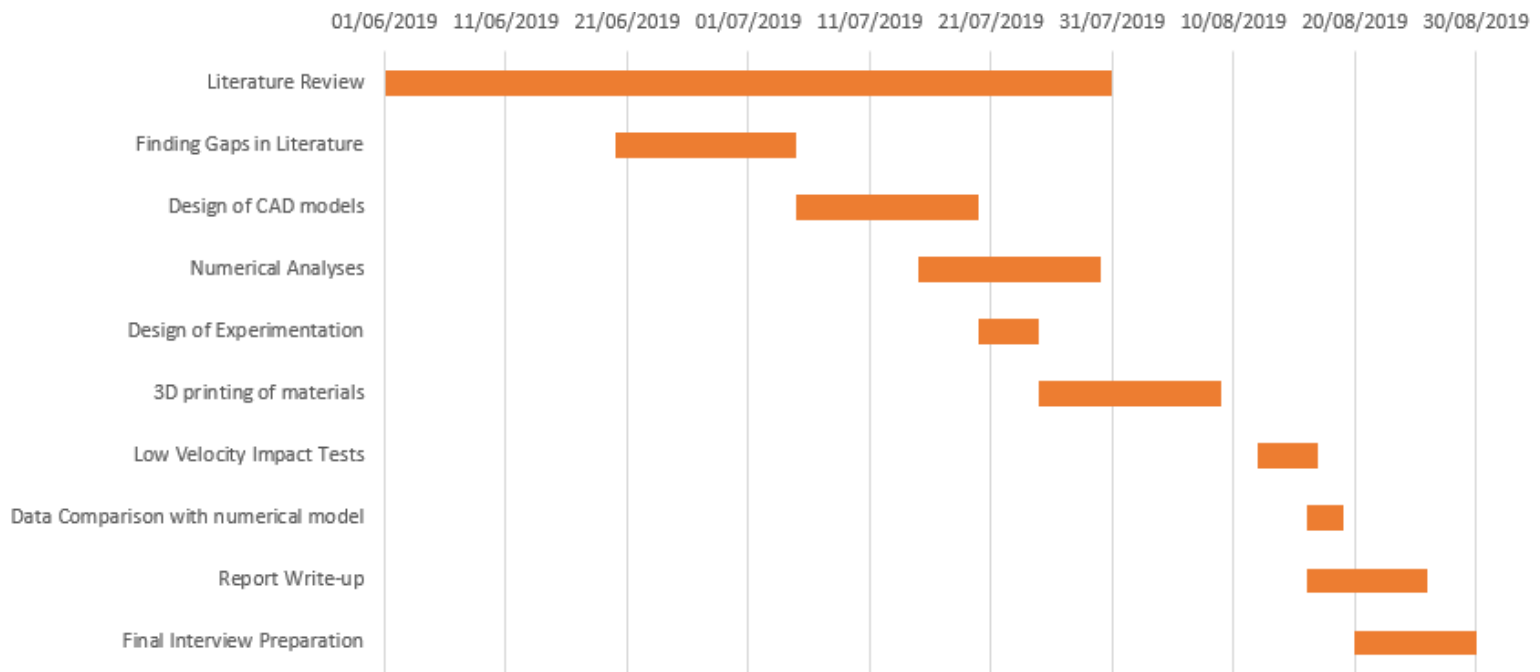
| | |
|---|----|
| Figure 1. On applying tension and compression: (a) non auxetic material; (b) auxetic material (Novak, Vesenjak and Ren, 2016) | 10 |
| Figure 2. Schematic of a Sandwich Structure (Sivák, Delyová and Diabelková, 2017) | 11 |
| Figure 3. Milton-Ashaby Map of Auxetic Structures (Christensen et al., 2015) | 12 |
| Figure 4. Different Auxetic Lattice configurations: (a) re-entrant hexagonal, (b) star, (c) double arrowhead, and (d) chiral (Gao et al., 2019)..... | 12 |
| Figure 5. Schematic of re-entrant hexagon showing auxetic behaviour (Ren et al., 2018)..... | 13 |
| Figure 6. Schematic of a 3D re-entrant cell (Yang et al., 2015) | 13 |
| Figure 7. Schematic of a double arrowhead cell (Qiao and Chen, 2015)..... | 14 |
| Figure 8. Schematic of rotating square unit cell; l – length of square; θ – angle between squares (Grima et al., 2008) | 15 |
| Figure 9. Auxetic Structure without deformation (left); Auxetic Structure with deformation (right) using rotating triangles as unit cell (Rafsanjani and Pasini, 2016)..... | 15 |
| Figure 10. Auxetic Structure with Chiral unit cell in red (Prall and Lakes, 1997)..... | 16 |
| Figure 11. a) crumpled paper sheet through varied strain levels; b) graphene sheet with 3% defects through varied strain levels (Grima et al., 2014)..... | 17 |
| Figure 12. Compression Results; a) conventional material; b) auxetic material (Alderson et al., 1999) | 17 |
| Figure 13. Deformation with bending: a) saddle shape (non-auxetic); b) dome shape (auxetic) (Alderson et al., 2010)..... | 18 |
| Figure 14. Schematic of auxetic structure showing variable permeability (Grima and Caruana-Gauci, 2013)..... | 19 |
| Figure 15. Schematic of (1) honeycomb; (2) re-entrant; (3) double arrowhead cells..... | 23 |
| Figure 16. (a) Double Arrowhead; (b) Re-entrant; (c) Honeycomb core structures designed in CAD.. | 24 |

| | |
|--|----|
| Figure 17. In clockwise order from top left; re-entrant(Onyx); double arrowhead(Onyx); honeycomb(Onyx); honeycomb(Nylon); double arrowhead(Nylon); re-entrant(Nylon) samples | 26 |
| Figure 18. Schematic of the base of the Drop-weight testing machine | 27 |
| Figure 19. (a) Testing Parameter Controller; (b) Impact test machine..... | 28 |
| Figure 20. Force vs Displacement Curves for the tested samples. (a)Nylon DA; (b)Onyx DA; (c)Nylon Re-entrant; (d)Onyx Re-entrant; (e)Nylon Honeycomb; (f)Onyx Honeycomb | 30 |
| Figure 21. Force vs Time Curves for the tested samples. (a)Nylon DA; (b)Onyx DA; (c)Nylon Re-entrant; (d)Onyx Re-entrant; (e)Nylon Honeycomb; (f)Onyx Honeycomb..... | 31 |
| Figure 22. (a) Nylon Test specimens after the impact test; (b) Onyx Test specimens after the impact test | 32 |
| Figure 23. Crashworthiness Performance Indicators. (a)Peak Indentation; (b)Crush Force Efficiency; (c)Peak Energy Absorbed; (d)Ductility Index | 33 |
| Figure 24. Printing defect caused by a dislocation | 35 |
| Figure 25. Printing error caused by broken Bowden Tube | 36 |

List of Equations

| | | |
|---|-------------|----|
| $H \propto E1 - v2\gamma$ | Eq. 1 | 18 |
| Relative Density _{double arrowhead} = $\frac{\rho}{\rho_s} = t(\sin\theta_1 + \sin\theta_2)d \sin(\theta_1 - \theta_2)$ | Eq. 2 | 23 |
| Poisson's Ratio _{double arrowhead} = $\nu = -\frac{1}{\tan\theta_1 \tan\theta_2}$ | Eq. 3.. | 23 |
| Relative Density _{re-entrant/honeycomb} = $\frac{\rho}{\rho_s} = \frac{\frac{t}{l(\frac{h}{l}+2)}}{2\cos\theta(\frac{h}{l}+\sin\theta)}$ | Eq. 4 ... | 24 |
| Poisson's Ratio _{re-entrant/honeycomb} = $\nu = \frac{\cos\theta(\frac{h}{l}+\sin\theta)}{\tan\theta}$ | Eq. 5..... | 24 |
| Ductility Index = $Total\ Energy - Absorbed \frac{Energy}{Absorbed} Energy$ | Eq. 6..... | 34 |

Work Package



Nomenclature

Symbols:

| | |
|----------|-----------------------------------|
| G | shear modulus (Pa) |
| ρ | mass density (Kg/m ³) |
| E | young's modulus (Pa) |
| B | bulk modulus (Pa) |
| l | length of square (mm) |
| H | material hardness |
| γ | hertzian indentation |
| ρ_s | bulk material density |
| Θ | angle between lines |
| ν | poisson's ratio |

Abbreviations:

| | |
|------|--|
| NPR | negative poisson's ratio |
| 3D | three-dimensional |
| 2D | two-dimensional |
| PR | poisson's ratio |
| DA | double arrowhead |
| FEM | finite element method |
| AM | additive manufacturing |
| CAD | computer aided design |
| EBM | electron beam melting |
| SLM | selective laser melting |
| ASTM | American society for testing and materials |
| CFE | Crush Force Efficiency |

1.0 Introduction

Technological Breakthroughs in Material Sciences are a result of constant demand of superior material requirements in Industries like Aerospace, Automobile, Aviation and Spacecraft. The following report highlights one such breakthrough in the form of materials possessing negative Poisson's ratio (NPR), which are also known as Auxetic Materials. These materials can be seen in nature (Wollner, Vanorio and Kiss, 2018) as well as can be synthetically (Hou et al., 2018) created. Different parameters in the form of geometry (Wang, 2019) and material properties (Panowicz and Miedzińska, 2012) have been studied that are responsible for the phenomenon. The report aims to find a relation between various parameters including materials, geometry, properties and their effective applications. Most of the auxetic materials showcase superior qualities, but only handful of these have been produced for industrial applications at present as the complex geometry of these structures makes it a challenge to mass produce. The challenges that arise while producing them will be also discussed in the report.

When an auxetic material is subjected to tensile longitudinal stresses, it laterally expands, unlike materials with positive Poisson's ratio which shrink and vice versa when subjected to compressive stresses (Prawoto, 2012), also depicted in Figure 1.

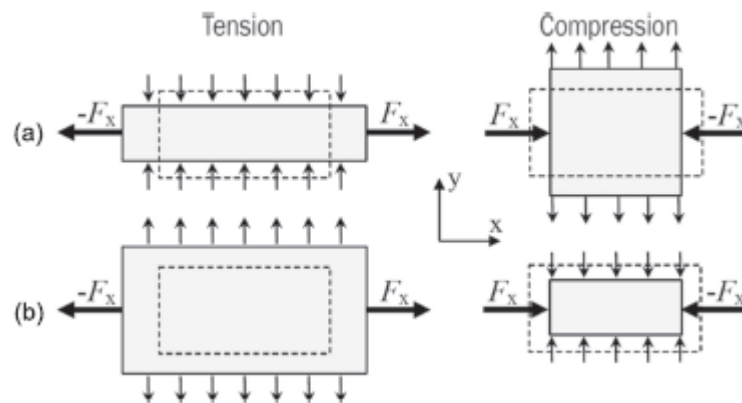


Figure 1. On applying tension and compression: (a) non auxetic material; (b) auxetic material (Novak, Vesenjajk and Ren, 2016)

Characterisation techniques have been studied from various research works to find out what makes these materials superior with desirable properties like superior shear resistance (Choi and Lakes, 1992), fracture resistance (Choi and Lakes, 1996), energy absorption performance (Imbalzano et al., 2016), blast resistance (Imbalzano et al., 2018), indentation resistance (Argatov, Guinovart-Díaz and Sabina, 2012) and variable permeability (Alderson et al., 2000).

The superior properties mentioned make auxetic materials suitable for applications like seat cushions (Wang and Lakes, 2002), stent grafts (Ali and Rehman, 2015), piezoelectric sensors (Ferguson et al., 2018), non-pneumatic tires (Jin et al., 2018), smart filters (Alderson et al., 2000),

auxetic textiles (Zeng, Hu and Zhou, 2017) and magnetic auxetic systems (Grima et al., 2013). Out of all the studies carried out in the following area, very limited work has been applicable practically. It remains to be seen that even after possessing such superior qualities in comparison with conventional structures, why the following groups of materials are not getting exploited in the industry.

Sandwich structures are regarded as a type of multi-layered composite structures, that are being widely used in aerospace, automotive and marine industries as they have high stiffness to weight ratio, superb thermal insulation and good energy absorption capabilities (Schaedler and Carter, 2016). The structure comprises of a lightweight cored structure sandwiched between thin but stiff outer facing sheets providing high bending stiffness and buckling resistance (Andrews, Gibson and Ashby, 1999).

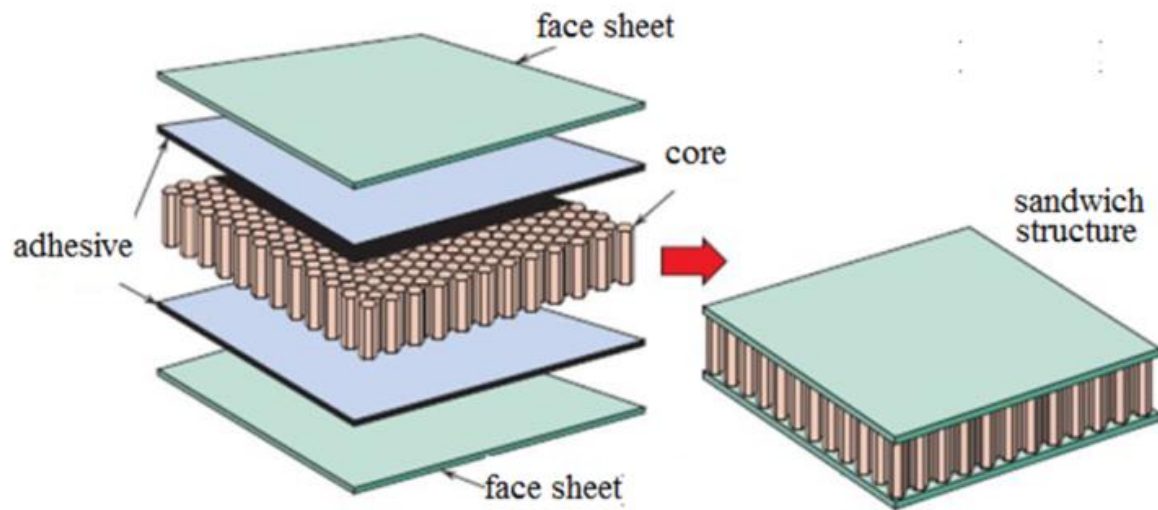


Figure 2. Schematic of a Sandwich Structure (Sivák, Delyová and Diabelková, 2017)

The objective of the study is to fill the gap in literature of auxetic structures manufactured using advanced additive manufacturing, to enhance their mechanical characteristics based on the specific needs of the industry. A comparison of re-entrant, double arrowhead and hexagonal cellular structures using 2 different materials (Nylon and Onyx) subjected to low velocity impacts would help to understand the key mechanical characteristics of these materials so they can be optimised as per the industry needs.

2.0 Literature Review

The following section will provide a review of literature of auxetic structures, their properties, applications, and their manufacturing techniques.

2.1 Cellular Materials

Cellular materials possess better thermal and mechanical properties on comparison with solid materials, like high energy absorption, damping, filters etc. These structures also showcase counter-intuitive results, that is expanding under co-axial load direction of tension and vice versa. A relation between auxetic materials and conventional materials is showcased using Milton-Ashaby map of auxetic structures (shear modulus (G), mass density (ρ), bulk modulus (B)) (Figure 3). The red pyramid covers property space of auxetic cellular structures and black ellipse shows properties of ordinary solids (Christensen et al., 2015).

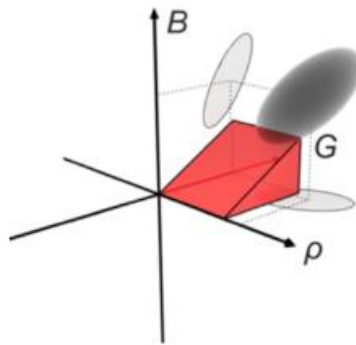


Figure 3. Milton-Ashaby Map of Auxetic Structures (Christensen et al., 2015)

The auxetic core is generally found as a type of cellular materials in the form of foams and periodic lattice structures. The auxetic cored sandwich structures are continuously being optimised in the form of material complexity and sandwich structure architecture because of increasing demand for improvement in aerodynamic, structural and thermal insulation performances in wide engineering applications (Yazdani Sarvestani et al., 2018). Some of the auxetic lattice structures with varying configurations are re-entrant hexagonal (Fu et al., 2016), star (Shokri Rad, Ahmad and Alias, 2015), double arrowhead (Qiao and Chen, 2015) and chiral (Xu et al., 2017) as depicted in Figure 4.

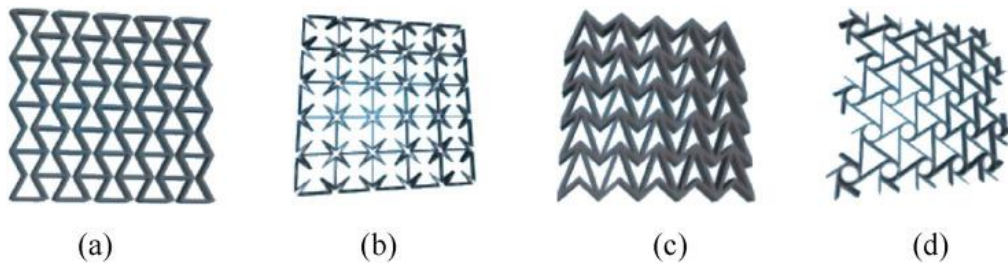


Figure 4. Different Auxetic Lattice configurations: (a) re-entrant hexagonal, (b) star, (c) double arrowhead, and (d) chiral (Gao et al., 2019)

Álvarez Elipe et al., 2012 selected numerous auxetic structures and compared their mechanical properties by using computer-aided design to infer that double arrowhead and re-entrant hexagonal structure possess highest Young's modulus among all auxetic structures under study.

2.1.1 Re-entrant Structures

A theoretical model of a re-entrant structure was developed in 2D that could detect elasticity of foams and honeycombs via hinging, flexure and stretching (Masters and Evans, 1996). Auxetic behaviour in these structures could be seen due to the ribs pivoting about the hinge for re-entrant hexagonal system (Alderson and Alderson, 2007). A schematic of 2D honeycomb with re-entrant structure (hexagon) can be seen in Figure 5.

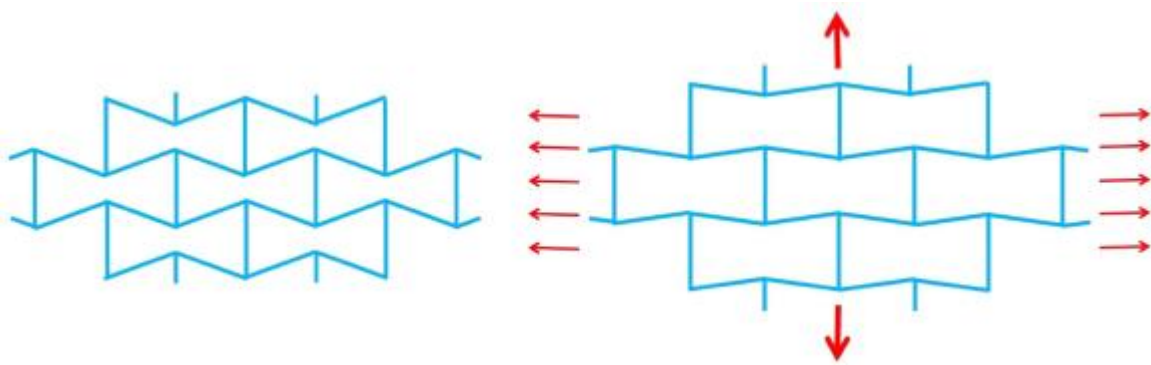


Figure 5. Schematic of re-entrant hexagon showing auxetic behaviour (Ren et al., 2018)

Formulating the theory of 2D re-entrant structures, a 3D re-entrant structure with hexagonal lattice pattern that shows NPR in different directions was designed by Schwerdtfeger et al. (2010). Re-entrant structures possess anisotropic nature, that is, showing different properties across different axes. Thus, Yang et al. (2015) presented a 3D orthotropic re-entrant structure by the unit

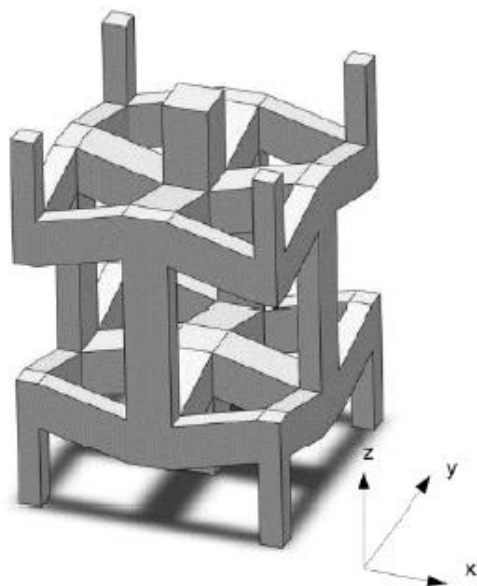


Figure 6. Schematic of a 3D re-entrant cell (Yang et al., 2015)

cell as shown in Figure 6. Yang et al. (2015) also concluded that the re-entrant angle and characteristic strut ratio could control the mechanical properties of auxetic re-entrant structures. A 3D augmented model was demonstrated by Li et al. (2017) which could possess multiple poisson's ratio by adjusting the model from negative to positive values. Similarly, an auxetic multi-entrant honeycomb structure was proposed by Harkati et al. (2017) showing variable poisson's ratio and stiffness. A model with hexagonal honeycombs showing zero PR was proposed by Grima et al. (2010) that enhanced the stiffness of the model.

2.1.2 Double Arrowhead Structures

Double arrowhead (DA) structures possessing negative poisson's ratio was first showcased by Larsen et al. (1997). He designed a two-dimensional symmetric unit cell consisting of four beams. Two beams are short inclined beams and the other two are long inclined beams making a closed shape as shown in Figure 7.

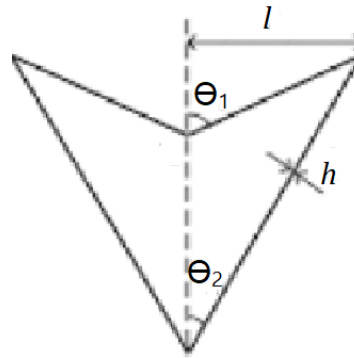


Figure 7. Schematic of a double arrowhead cell (Qiao and Chen, 2015)

Wang et al. (2018) proposed a three-dimensional double arrowhead sandwich structure as a substitute to protective solid plate in military vehicles. The auxetic structure was optimised to absorb more blast energy. The 3D double arrowhead core showcased isotropic mechanical behaviour in contrast to anisotropic mechanical behaviour of the 2D double arrowhead structures. The 3D double arrowhead sandwich structure provided better protection and lighter weight on comparison with square honeycomb sandwich structure. The following structure was also used to enhance the crashworthiness performance of a crash box (Zhou et al., 2016) and improve vehicle ride comfort by implementing the DA cores to suspension jounce bumpers (Wang et al., 2016).

2.1.3 Polygon Rotating Models

Auxeticity can be also achieved using closed polygons connected like re-entrant structures. In one such study, squares were used as polygons with the adjoining vertices of adjacent squares connected using hinges (Grima et al., 2008) as can be seen in Figure 8. Similarly, rotating triangles (Grima and Evans, 2006) and rotating rhombi (Attard and Grima, 2008) with similar orientation as

that of rotating square were used to achieve auxeticity which can be implemented into real applications. For reference, formation and deformation of auxetic structure using rotating triangles as unit cell are shown in Figure 9. Based on the orientation of these structures, the PR can be both positive and negative as these structures are anisotropic in nature, which is further dependent on unit cell configuration.

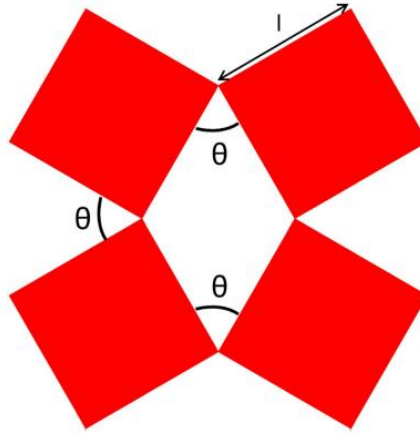


Figure 8. Schematic of rotating square unit cell; l – length of square; θ – angle between squares (Grima et al., 2008)

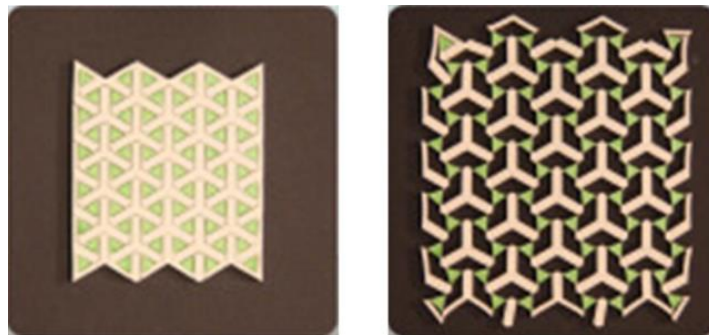


Figure 9. Auxetic Structure without deformation (left); Auxetic Structure with deformation (right) using rotating triangles as unit cell (Rafsanjani and Pasini, 2016)

2.1.4 Chiral Models

Chiral Models are also a type of cellular auxetic structures. Chiral, by definition, means a structure whose mirror image is non – superimposable on the original structure. But the terminology is also used to demonstrate a spinning property. An experiment was carried out using 2D honeycombed chiral, which resulted with PR of -1 (Prall and Lakes, 1997). A schematic of the auxetic structure of the same experiment with basic chiral units is shown in Figure 10, in which straight ligaments are connected to central node.

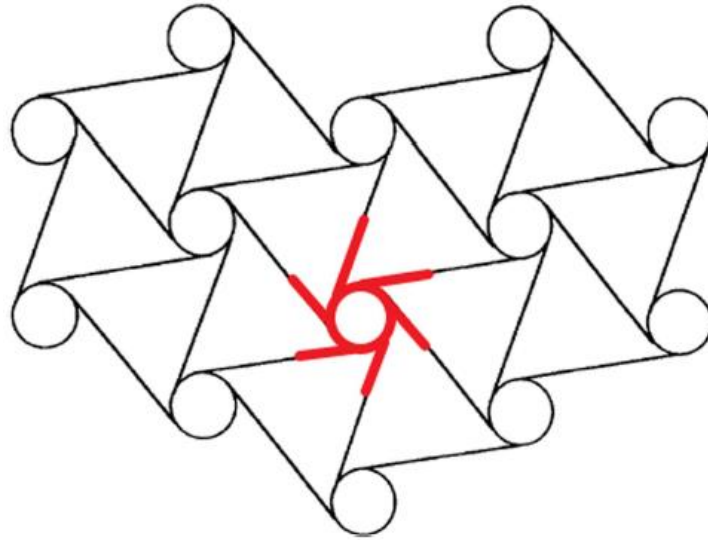


Figure 10. Auxetic Structure with Chiral unit cell in red (Prall and Lakes, 1997)

A similar study on Chiral structures was conducted by Gatt et al. (2013) on the mechanical behaviour of flexing chiral systems through finite element methods (FEM) and analytics. The results inferred that material characteristics and geometrical properties of the parent materials have major impact on mechanical behaviour of flexing chiral systems. In other words, the PR of these structures is governed by the ratio of ligament thickness and length. Gatt et al. (2013) concluded that without affecting the PR, the rigidity of chiral system can be adjusted by varying the relative stiffness in ligament structures.

2.1.5 Crumpled sheet models

These models have recently been discovered to show NPR. Alderson et al. (2012) showcased manufacturing procedure of flat, thin and foamed auxetic sheets using uniaxial compression, which was characterised using PR measurements and optical microscopy. Hall et al. (2008) mixed multi-walled and single walled nanotubes to find out that the PR of produced nanotube sheets has been converted from positive to negative values including high increase in sheet toughness, modulus and strength. Similarly, a study was conducted by Scarpa et al. (2009) to study elastic mechanical behaviour of layered graphene sheets with numerical and analytical techniques. It was inferred from the study that shear loading possessed equivalent auxetic characteristic when bond material is considered as an equivalent isotropic material. In a separate study, it was showcased that conformation of Graphene sheets could be modified with some molecular scale defects as studied through molecular dynamic simulations which introduced NPR in the structure (Grima et al., 2014). A schematic of the crumpled paper sheet and graphene sheet is shown in Figure 11 demonstrating the auxetic behaviour of crumpled sheet conformation.

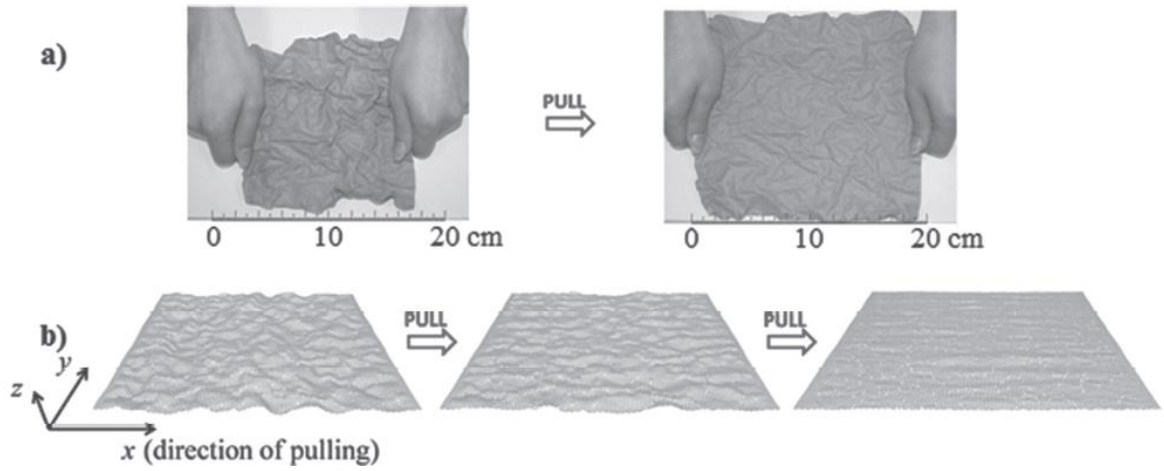


Figure 11. a) crumpled paper sheet through varied strain levels; b) graphene sheet with 3% defects through varied strain levels (Grima et al., 2014)

2.2 Auxetic Material Properties

Auxetic Structures and Materials showcase counter-intuitive deformation characteristics providing superior properties on comparison with conventional structures. Key properties of Auxetic Structures are demonstrated in the present section.

2.2.1 Indentation Resistance

On application of local compression, a conventional material with positive PR would expand laterally in a direction perpendicular to the applied load (Evans and Alderson, 2000). On the contrary, an indentation would appear on the surface on subject to compression in auxetic materials. The following phenomenon is best described in Figure 12.

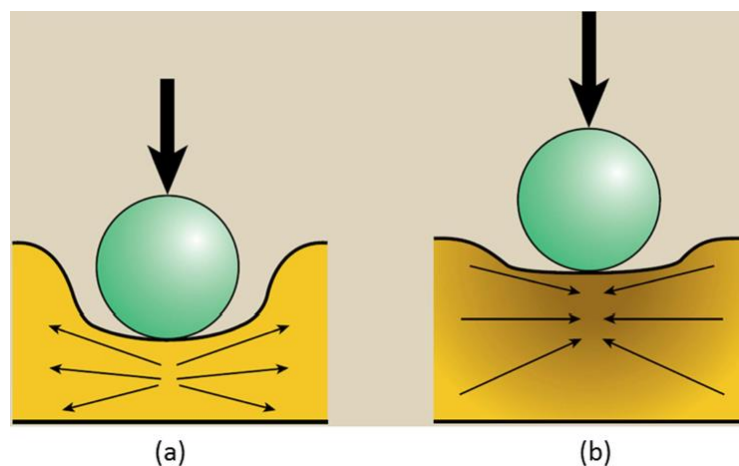


Figure 12. Compression Results; a) conventional material; b) auxetic material (Alderson et al., 1999)

Lakes et al. (1993) made a revelation that foams when subjected to indentation resistance showed auxetic behaviour irrespective of either positive or negative PR using holographic interferometry. As per the theory of Elasticity, material hardness (H), is related to indentation resistance, which can be directly correlated with the Poisson's ratio using the equation:

$$H \propto \left[\frac{E}{1-\nu^2} \right]^\gamma \quad \text{Eq. 1}$$

Where E = *Young's Modulus*; ν = PR; $\gamma = 2/3$ or 1 (Hertzian indentation or pressure distribution respectively)

From the equation above, indentation resistance goes to infinity as PR tends to 1 or -1 (Critchley et al., 2013). In case of 3D isotropic solids with maximum PR of 0.5, the indentation resistance is significantly lowered. However, 2D isotropic systems possess maximum PR of 1, resulting in infinite hardness (Tretiakov and Wojciechowski, 2012).

2.2.2 Synclasticity

Conventional materials, when subjected to bending moment perpendicular to the longitudinal axis possess saddle shape. On the other hand, auxetic materials exhibit a dome shape as depicted in Figure 13.

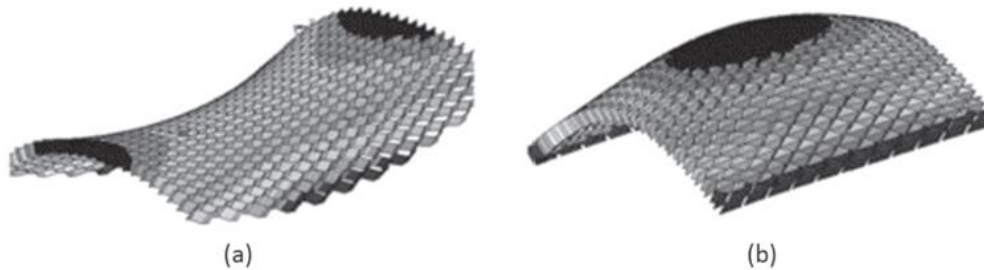


Figure 13. Deformation with bending: a) saddle shape (non-auxetic); b) dome shape (auxetic) (Alderson et al., 2010)

The dome shaped deformation in case of auxetic structure is referred to as Synclasticity. The following characteristic is quite useful given the fact that dome shaped auxetic structures can be fabricated by just damaging rather than using further machining operations (Lorato et al., 2010).

2.2.3 Variable permeability

Majority of auxetic structures are porous microstructures, the size of these pores varies when subjected to deformation in the form of compression or tension. The following characteristic can be utilised to make it suitable for filter applications. Figure 14 demonstrates the phenomenon discussed. In one such study, it was illustrated that auxetic material can offer high filter performance right from nano-scale to the macro-scale because of their rare features and characteristics (Alderson et al., 2001). Moving further, Alderson et al. (2007) experimented on transmission tests of glass beads on auxetic foams showcasing the benefits in mass transportation applications with scale ranging from macro to nano-filters.

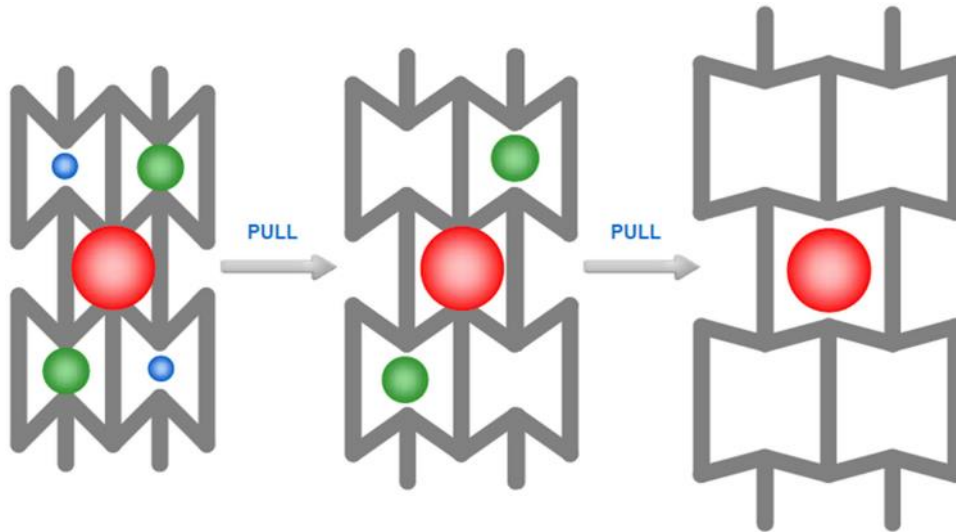


Figure 14. Schematic of auxetic structure showing variable permeability (Grima and Caruana-Gauci, 2013)

2.2.4 Energy absorption

Auxetic materials possess superior energy absorption characteristics as compared with conventional materials. Yang et al. (2013) compared the ballistic resistance of aluminium foamed cored panels and auxetic sandwich panels using extensive numerical simulations. It was seen that auxetic sandwich panels possessed superior ballistic resistance on comparison with aluminium foamed core panels due to material concentration at the area of impact because of its auxetic behaviour. Mohsenizadeh et al. (2015), Imbalzano et al. (2018) conducted similar studies comparing an auxetic cored sandwich panel with equivalent honeycomb structure using crashworthiness indicators and blast resistance performance indicators. The results suggested that auxetic cored structure absorbed twice the amount of impulsive energy with plastic deformation and significant improvement in shockwave mitigation in comparison with the equivalent honeycomb structure.

2.3 Auxetic Structure Applications

Auxetic structures possess counter-intuitive behaviour when subjected to deformation, making the following characteristics extremely desirable with many potential applications. Some applications are mentioned in the following section.

2.3.1 Protective Devices

Auxetic structures exhibit distinctive characteristics that make them extremely suitable for sports protective devices like gloves, pads, mats and helmet (Saxena, Das and Calius, 2016). Auxetic structures can be used to produce impact protection products, providing significant support conformability and better energy absorption properties for thin and light products. Similarly, an auxetic honeycomb could be used to manufacture Helmet and similar applications, with non-auxetic and auxetic foams to be used for the application of running shoes and protective crash pads (Sanami et al., 2014). Perforated sheets and foamed auxetics can also be used for protective sports gears and products.

2.3.2 Auxetic Nails

Choi et al. (1991) ideated that auxetic behaviour could be most suitable for fastening applications, as it would be simple to insert the fastener as auxetics contract laterally under compression, at the same time, difficult to pull out as auxetics expand laterally under tension. Until now, auxetic fasteners were a theoretical concept until Ren et al. (2018), who designed, produced and tested them. It was concluded that auxetic fasteners did not always possess superior insertion and pull out performance in comparison with conventional nails. Further experimentation needs to be done before using auxetic fasteners applications.

2.3.3 Smart Piezoelectric Sensors

Auxetic structures have the properties required to improve the performance characteristics of piezoelectric sensors by a considerable margin. Piezoelectric composites consist of ceramic rods enclosed inside a polymer matrix that function by converting the mechanical stresses induced on the rods into electrical impulse and vice versa. Galfenol, a smart auxetic material, made of iron and gallium possessed magneto-elastic characteristics suitable for piezoelectric sensors was investigated by Raghunath et al. (2016).

Ferguson et al. (2018) developed piezoelectric energy harvester consisting of an auxetic substrate bonded together with the piezoelectric element to increase the power output while tapping strain

energy. The energy harvester with auxetic substrate was manufactured and characterised to find out that the peak power produced by auxetic energy harvester was nearly 14 times the peak output produced by the conventional harvester.

2.3.4 Textile

Textile products possessing auxeticity are popular in the market due to the characteristics in the form of wear resistance, drapeability, high energy absorption and high-volume change (Alderson et al., 2012). Auxetic behaviour in textile materials is introduced using two common techniques. The first technique is to knit and weave the textile directly using auxetic based fibres (Simkins et al., 2005). The other technique is to use the conventional non auxetic fibre, but the orientation of the knit is designed as such which makes the final textile product auxetic in nature (Alderson et al., 2012).

2.4 Auxetic Core Fabrication

A major setback for complex structures such as honeycomb sandwich structures is their mass production. The issues related with continuous manufacturing of these complex hexagonal honeycomb structures is stated by Fan et al. (2009). A similar thermoforming process has been incorporated and discussed by Bratfisch et al. (2007). Unlike thermoforming techniques, some studies also used bulk material where structure is cut through leading to both material and energy wastage. Due to these constraints, that is time, money (material) and energy, a new technique is devised to ease the production process. 3D printing or additive manufacturing (AM) is capable to produce these materials efficiently as it provides substantial advantages in the form of geometrical freedom, material waste reduction, high precision and short processing time. AM is a technique to make a physical model from a CAD model, by forming layer by layer of the given material in succession. On comparing it with thermoforming techniques, AM is a far better technique since there are no geometric limitations that becomes helpful in to test varying geometries with multiple material options.

3D printing machines are getting affordable with the advancements in technology making them easily available, which has also helped in increasing the production rate of the sandwich panels. Combination of materials and geometric designs are being designed, produced and tested through numerous AM techniques. Electron Beam melting (EBM) technique was used to manufacture variety of metal components for testing (Yang et al., 2015). The components manufactured through EBM manufacturing process possessed high accuracy with respect to their CAD model. In a similar study, three geometries of honeycomb cells were produced using 3D inkjet printers for the shape recovery experimentation with dimensional accuracy of 0.2mm (Yap and Yeong, 2015).

Alternatively, Fused deposition modelling technique was used using inkjet 3D printer to produce sandwich composite structures (Dikshit et al., 2016).

The structures produced through the 3D printing AM techniques are considered to possess anisotropic behaviour as it is fabricated through layer by layer process. The following fact should be addressed, and the same orientation be checked during fabrication to prevent influence of mechanical properties (Li and Wang, 2017). Similarly, Alomarah et al. (2017) while using sintered laser melting (SLM) to produce honeycomb structures with aluminium and silicon, carried out similar preventive measures to check the orientation before fabrication.

3.0 Project Objectives

The aim of the project is the comparison of performance of auxetic cores in the form of hexagonal, re-entrant and double arrowhead structures, subjected to low velocity impacts.

A proposed methodology based on the studied literature is as follows:

- Selecting auxetic structures by their geometry, material type.
- Designing CAD models for selected auxetic structures
- Manufacturing the auxetic structures with different materials through 3D printing process using Markforged printers.
- To perform low velocity impact load tests to find out the impact resistance properties of the structure.
- To compare and discuss the results with literature.

4.0 Experimental Procedure

4.1 Unit Cell Design

The auxetic cell configurations selected for the project as per the literature were re-entrant and double arrowhead as they show superior indentation resistance. Honeycomb cell was also chosen to compare the results of auxetic and non-auxetic structures. The schematic of the following chosen configurations is depicted in Figure.

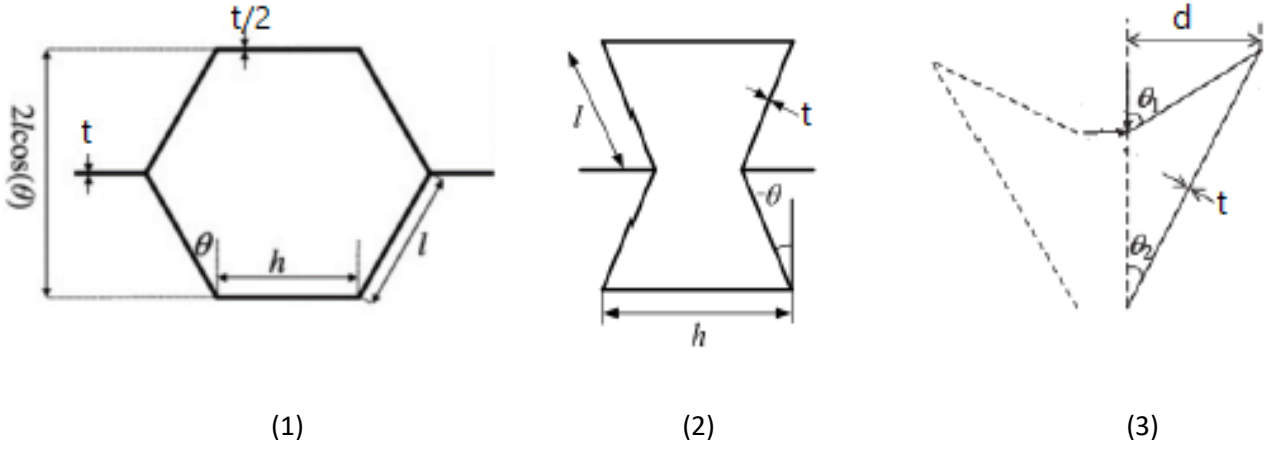


Figure 15. Schematic of (1) honeycomb; (2) re-entrant; (3) double arrowhead cells

Table 1 Design Parameters

| Design Parameter | Description |
|------------------|--|
| H | Vertical strut length |
| l | Inclined strut length |
| t | Strut thickness |
| Θ | Angle of inclined strut |
| d | Half width of double arrowhead cell |
| Θ_1 | Half angle between short inclined struts |
| Θ_2 | Half angle between long inclined struts |

The design parameters shown in Table 1 are the driving factors in influencing the poisson's ratio and relative density which further influence the mechanical characteristics of the core structure. It also should be kept in mind that poisson's ratio is anisotropic in nature in auxetic cells. Relative Density of a core is the ratio of the density of the designed core to the density of the bulk material. It evaluates the material utilization of the designed core. The design parameters were optimised to give negative poisson's ratio for re-entrant and double arrowhead cells and positive poisson's ratio for hexagonal cell. The poisson's ratio and relative density for double arrowhead (Qiao and Chen, 2015), re-entrant and honeycomb cells (Gibson et al., 1982) can be calculated using the equations mentioned.

$$\text{Relative Density}_{\text{double arrowhead}} = \frac{\rho}{\rho_s} = \frac{t(\sin\theta_1 + \sin\theta_2)}{d \sin(\theta_1 - \theta_2)} \quad \text{Eq. 2}$$

$$\text{Poisson's Ratio}_{\text{double arrowhead}} = \nu = \frac{-1}{\tan\theta_1 \tan\theta_2} \quad \text{Eq. 3}$$

$$\text{Relative Density}_{\text{re-entrant/honeycomb}} = \frac{\rho}{\rho_s} = \frac{\frac{t}{l(\frac{h}{l}+2)}}{2\cos\theta(\frac{h}{l}+\sin\theta)} \quad \text{Eq. 4}$$

$$\text{Poisson's Ratio}_{\text{re-entrant/honeycomb}} = \nu = \frac{(\cos\theta)}{(\frac{h}{l}+\sin\theta)\tan\theta} \quad \text{Eq. 5}$$

4.2 Sample Design

Table 2 Design Parameters of Unit Cell

| Cell Design | h (mm) | l (mm) | t (mm) | $\Theta(^{\circ})$ | Poisson's Ratio | Relative Density |
|------------------|-----------|-----------|----------------------|----------------------|-----------------|------------------|
| Honeycomb | 8.59 | 5.14 | 1.1 | 30 | 0.69 | 0.21 |
| Re-entrant | 6.6 | 7.34 | 1.1 | 20 | -4.63 | 0.41 |
| | d (mm) | t (mm) | $\Theta_1(^{\circ})$ | $\Theta_2(^{\circ})$ | Poisson's Ratio | Relative Density |
| Double Arrowhead | 7.5 | 1.1 | 80 | 35.51 | -0.24 | 0.32 |

Based on the design parameters shown in Table 2, CAD models were designed in Solidworks, (2018). The designs were constructed with core dimensions as 60mm x 60mm x 30mm which are also compliant with ASTM d3763 standards (ASTM D3763-10). Honeycomb and Re-entrant samples comprised of 4x5 cells and double arrowhead samples comprised of 4x3 cells having depth of 60 mm in out of plane configuration.

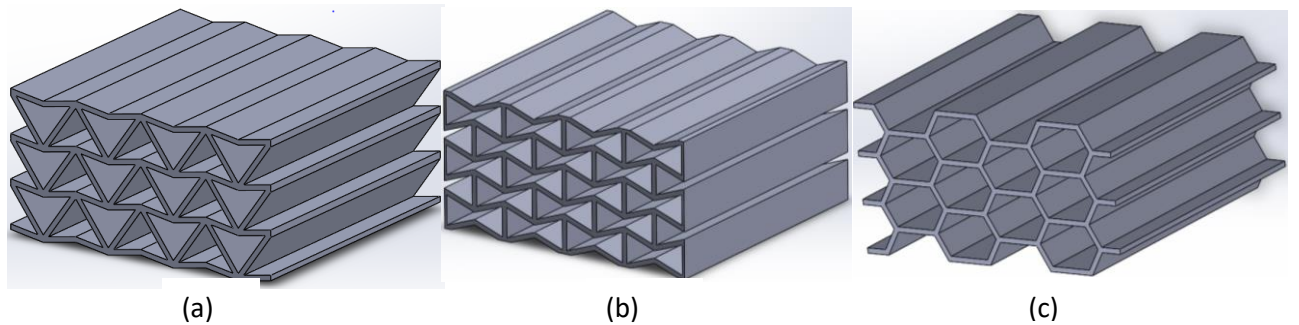


Figure 16. (a) Double Arrowhead; (b) Re-entrant; (c) Honeycomb core structures designed in CAD

4.3 Sample Production

The designed CAD models were manufactured using Markforged Mark 2 printers that uses layer by layer assembly through Fused Deposition Modelling process. After the CAD models were designed, they were imported to Eiger as .stl files, which is Markforged's printing software. There were several settings that could be used in the printing process as per user requirements. The print settings that were used in printing process can be seen in Table 3.

Table 3 Print Settings of Markforged Mark 2

| | |
|--------------------------|------------|
| Part Settings | |
| Scale | 1:1 |
| Use Supports | No |
| Expand Thin Features | No |
| Use Brim | Yes |
| Layer Height | 0.2mm |
| Material Settings | |
| Fill Pattern | Solid Fill |
| Fill Density | 100% |
| Roof & Floor Layers | 4 |
| Wall Layers | 1 |

Since the size of the samples were small, no supports were used while printing. Although the brim feature was used to hold the print to the bed. As for the print material, Nylon and Onyx were selected to print the samples, in which onyx is a type of Nylon reinforced with chopped carbon fibre to harden Nylon. The material properties were sourced from Markforged.com which can be seen in Table 4.

Table 4 Material Properties

| Material | Tensile Modulus (GPa) | Tensile Strength (MPa) | Flexural Strength (MPa) | Flexural Modulus (GPa) | Density (g/cm³) |
|-----------------|------------------------------|-------------------------------|--------------------------------|-------------------------------|-----------------------------------|
| Nylon | 0.94 | 54 | 32 | 0.84 | 1.10 |
| Onyx | 1.4 | 30 | 81 | 2.9 | 1.18 |

Based on the type of material selected for printing, Eiger Software calculates the dimensions of the print. Based on these calculations it shows beforehand the print time, material cost, final part mass and plastic volume. It took 6 hours on an average to print a single sample. The Markforged Mark Two print bed provided a build envelope of 320mm (bed length) x 132mm (bed width) x 160mm (depth) which could print 12 samples in a single print job consuming more than 72 hours to completion. But even a small fault in the printing process during the duration would mean loss of precious time, energy and material resources. So, it was decided to print a maximum of 4 samples at a point of time taking maximum of 24 hours to print. These details were used judiciously to set the printing schedule for the samples prepared.

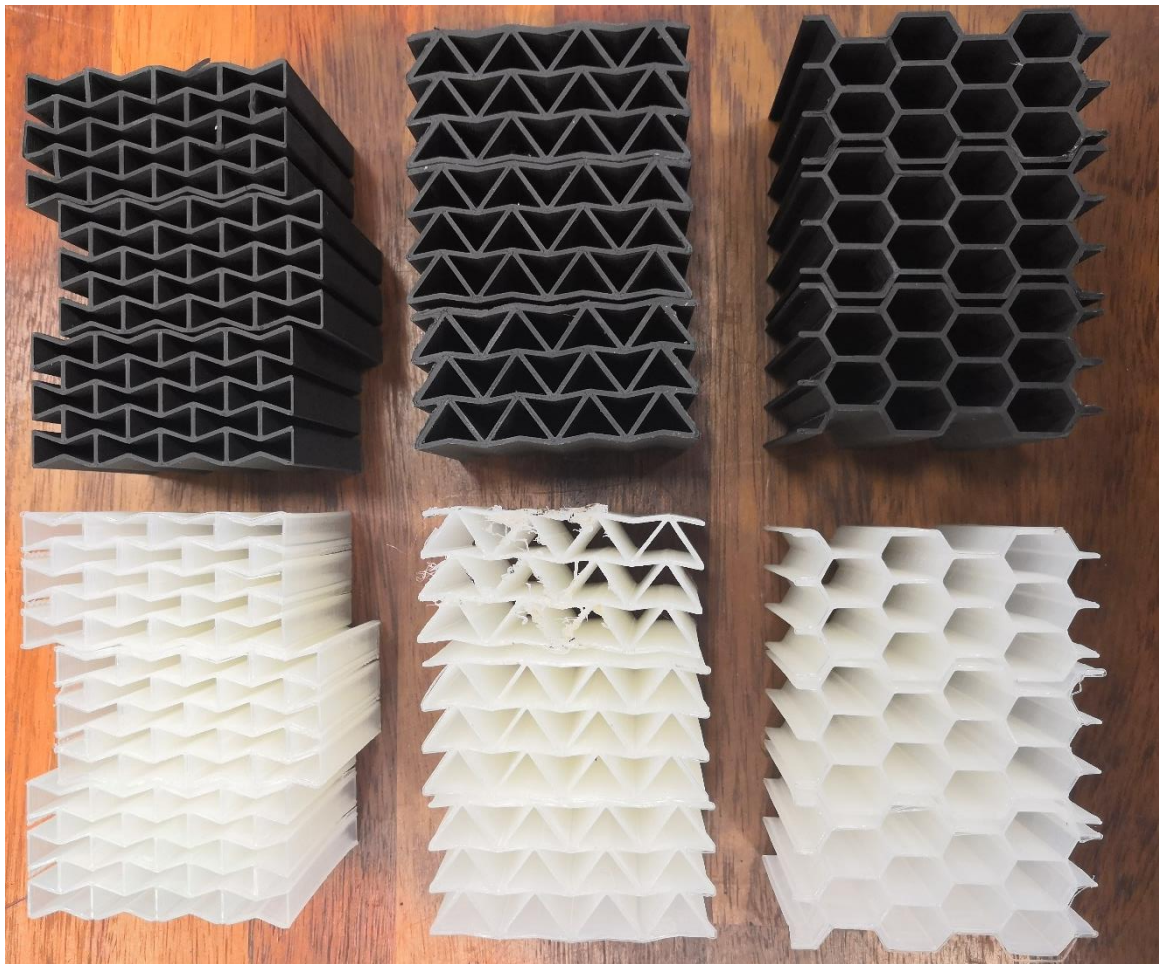


Figure 17. In clockwise order from top left; re-entrant(Onyx); double arrowhead(Onyx); honeycomb(Onyx); honeycomb(Nylon); double arrowhead(Nylon); re-entrant(Nylon) samples

As visible in the Figure 17, 18 samples were prepared in total with 3 samples each for every combination. The samples were checked after they were printed of their dimensions and masses to check the accuracy of the printing process with an accuracy of 0.01mm and 0.1g respectively.

4.4 Drop-weight impact Testing

The drop-weight test was carried out as per the ASTM d3763 standard. It is “the Standard Test Method for High Speed Puncture Properties of Plastics using Load and Displacement Sensors”. Fractovis Gravity Drop machine was used to carry out the impact tests. The Impact is a low velocity impact as the impact velocity is 3.43m/s, which is less than 10m/s (Shivakumar et al.,1985). The machine apparatus is relatively simple where an impactor is raised at a certain height to gain potential energy. A test specimen was kept at the base bed of the machine as can be seen in Figure 18.

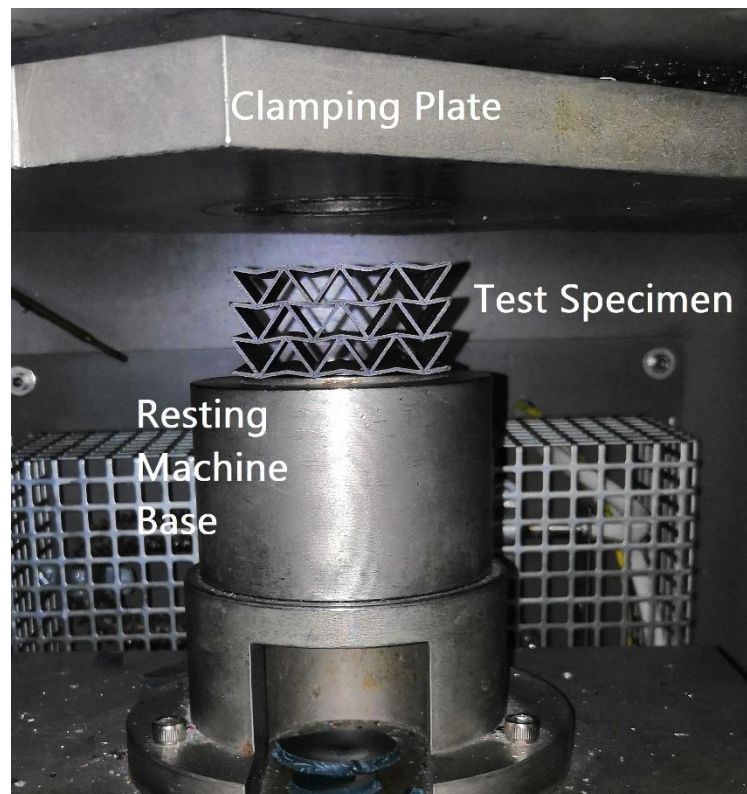


Figure 18. Schematic of the base of the Drop-weight testing machine

The test specimen was centred manually to keep the reliability of the test results high. After the specimen was centred, the safety door was closed after which the clamping plate descends automatically and clamps the specimen in between the rigid base and the clamping plate. This constrained the core to move about X and Y directions but could displace vertically about Z directions upon contact. Instrument and Test Parameters were set through the computer software to set the machine with an exception of impact mass which was adjusted manually. The impactor was a hemispherical striker with a striker diameter of 20mm. The impactor weight was 3.63Kgs which remained constant. Four 5Kg weight increments could be added on to the impactor

as per the test requirements. The impactor height could be adjusted up to 1 metre high from the rigid base.

Table 5 Equipment and Test Parameters

| Equipment parameters | |
|-----------------------|-----------|
| Number of Data points | 4000 |
| Sampling time | 6 μ s |
| Test time | 24ms |
| Striker range | 18.56kN |
| Working range | 6.187kN |
| Striker diameter | 20mm |
| Test parameters | |
| Mass | 8.630Kg |
| Impact velocity | 3.43m/s |
| Impact height | 0.6m |
| Impact energy | 50.78J |

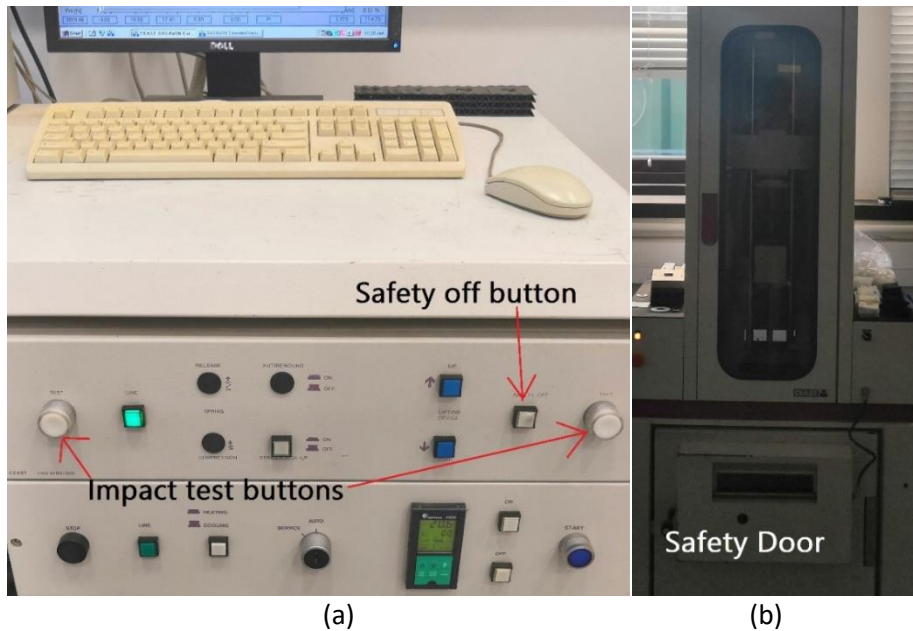


Figure 19. (a) Testing Parameter Controller; (b) Impact test machine

After the parameters were set, the safety off button was pressed as seen in Figure 19(a). The two impact test buttons were pressed simultaneously afterwards within 30 second time window to gravity-drop the impactor upon the test specimen. Once the test was completed, 4000 data points of the test with parameters including Force, Energy, Impact displacement and time were extracted from the machine software to interpret the results.

5.0 Results and Discussions

5.1 Experimental Results and Plots

Table 6 Experimental Results for 50.78J Impact Energy

| Shape | Material | Specimen | Peak Indentation(mm) | Peak Energy Absorbed(J) |
|------------------|----------|----------------|----------------------|-------------------------|
| Re-entrant | Onyx | 1 | 15.04 | 27.93 |
| | | 2 | 19.36 | 42.22 |
| | | 3 | 19.02 | 40.7 |
| | | <u>Average</u> | 17.80 | 36.95 |
| Hexagonal | Onyx | 1 | 25.69 | 24.17 |
| | | 2 | 22.39 | 23.52 |
| | | 4 | 21.88 | 22.57 |
| | | <u>Average</u> | 23.32 | 23.42 |
| Double Arrowhead | Onyx | 1 | 18.16 | 33.35 |
| | | 2 | 18.95 | 35.58 |
| | | 3 | 19.37 | 36.44 |
| | | <u>Average</u> | 18.82 | 35.12 |
| Re-entrant | Nylon | 1 | 18.28 | 24.87 |
| | | 2 | 17.65 | 15.88 |
| | | 3 | 19.82 | 29.77 |
| | | <u>Average</u> | 18.58 | 23.50 |
| Hexagonal | Nylon | 1 | 27.23 | 29.05 |
| | | 2 | 22.22 | 28.58 |
| | | 3 | 23.33 | 29.93 |
| | | <u>Average</u> | 24.26 | 29.18 |
| Double Arrowhead | Nylon | 1 | 13.98 | 25.1 |
| | | 2 | 15.19 | 22.83 |
| | | 3 | 15.4 | 24.99 |
| | | <u>Average</u> | 14.85 | 24.30 |

The data point that were collected from the Impact test experiment were used to plot Force-Displacement and Force-Time graphs to have a better understanding of the impact on all the samples.

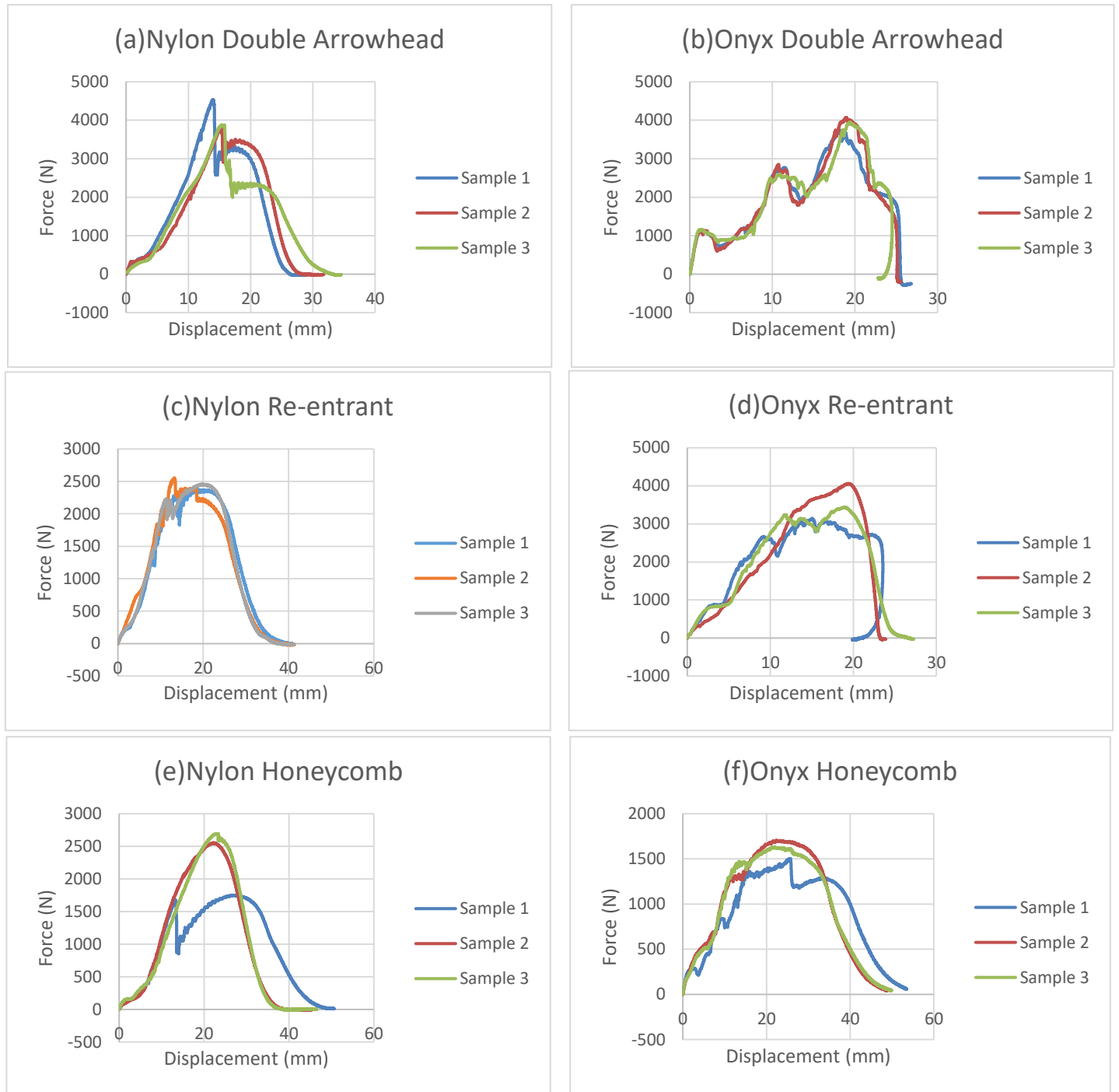


Figure 20. Force vs Displacement Curves for the tested samples. (a)Nylon DA; (b)Onyx DA; (c)Nylon Re-entrant; (d)Onyx Re-entrant; (e)Nylon Honeycomb; (f)Onyx Honeycomb

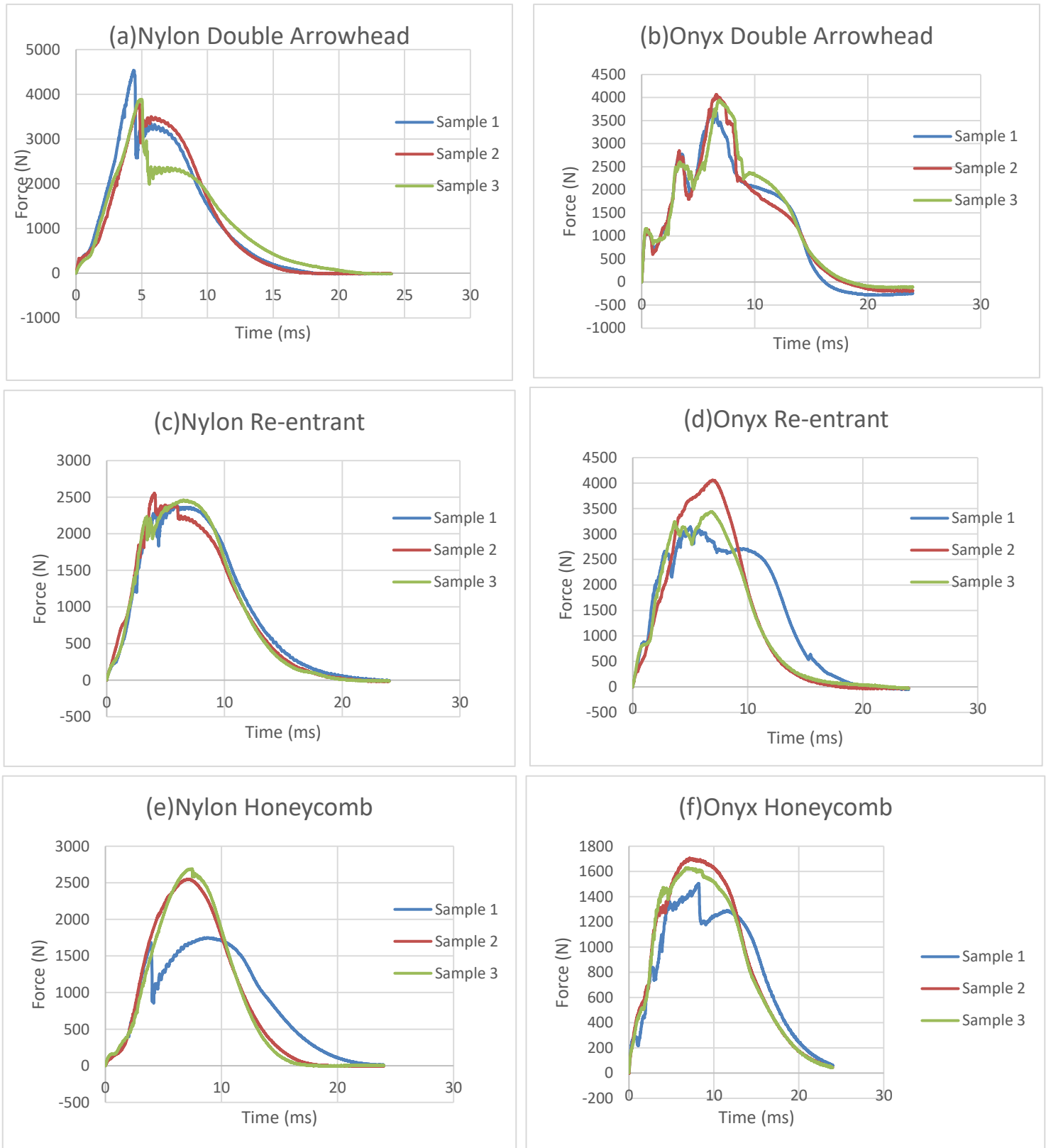


Figure 21. Force vs Time Curves for the tested samples. (a)Nylon DA; (b)Onyx DA; (c)Nylon Re-entrant; (d)Onyx Re-entrant; (e)Nylon Honeycomb; (f)Onyx Honeycomb

Impact behaviour in a composite structure as a result of drop weight test can occur in three ways, that are rebounding, perforation and penetration (Aktaş et al., 2009). Rebounding takes place when the impact energy is greater than the energy absorbed by the specimen which is the case in all the tests carried out. The impact energy is regarded as the total energy introduced to the specimen and absorbed energy as the one absorbed by the specimen during impact. In Force-Displacement curves as seen in Figure 20(b) (d) for some of the specimen, the decreasing displacement can be seen in the end with the curve folding on itself which exhibit rebound (Belingardi and Vadori, 2002). Also, the nylon samples possessed ductile behaviour and developed extended plasticity as no cracks could be seen on the specimen. The evidence of the behaviour could be checked with the linearity of the curve in the force-displacement graphs with no sudden drops. In case of Onyx samples, multiple peaks can be seen. The first peak shows the first contact between the impactor tip and the uppermost surface of the specimen which penetrates through the surface, creating a puncture. The second peak, which is at a much higher elevation creates a crack at the base of the Onyx specimens. The features are evident in Figure 22 where tested Onyx and Nylon samples can be seen with and without the cracks respectively.



(a)



(b)

Figure 22. (a) Nylon Test specimens after the impact test; (b) Onyx Test specimens after the impact test

5.2 Crashworthiness Performance Indicators

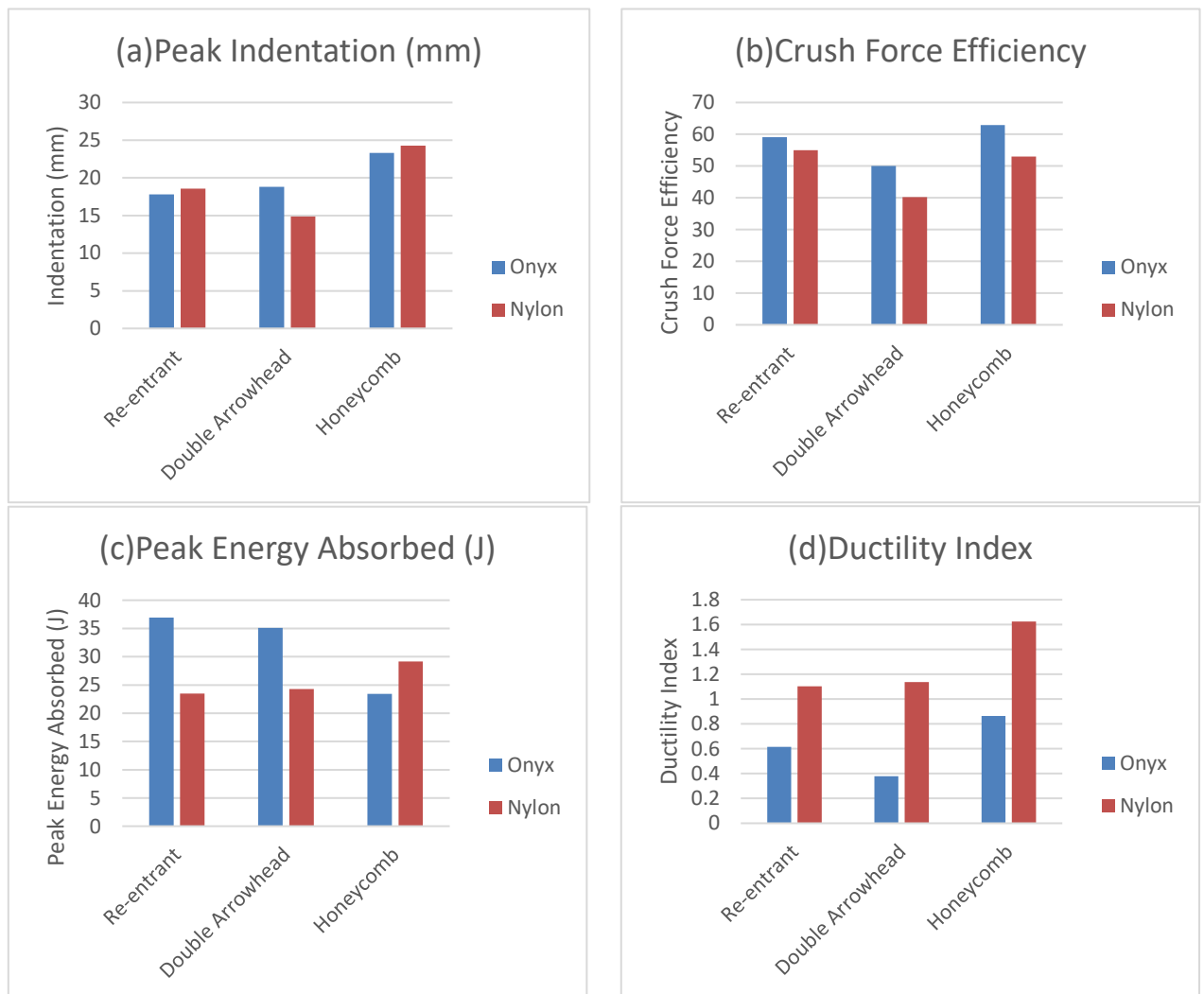


Figure 23. Crashworthiness Performance Indicators. (a)Peak Indentation; (b)Crush Force Efficiency; (c)Peak Energy Absorbed; (d)Ductility Index

Based on the experiment, as in Figure 23 (a), it was seen that double arrowhead made of nylon had minimum peak impact indentation, which was contrasting as the onyx samples showed better results for the other two specimens. The reason could be the number of specimens used for the testing which was limited to three specimens per sample due to time constraints.

The Crush Force Efficiency (CFE) is a crashworthiness performance indicator which conveys that higher the CFE, the energy absorption is more ideal in nature (Mohsenizadeh et al., 2015). It is calculated as a percentage of mean force upon peak impact force. Onyx Honeycomb structure possessed the maximum CFE with Nylon Double arrowhead having the minimum efficiency.

The graph with the peak energy absorption showed varied results on comparison with the literature presented. The anomaly can be seen in the Energy Absorption of Nylon Honeycomb structure which

is evidently more than the latter auxetic structures. It may be possible due to the defects that were incurred while manufacturing re-entrant and double arrowhead nylon samples with some warped faces.

Low ductility Index of a material is a direct attribute to brittle material. The ductility index of a core is calculated as:

$$\text{Ductility Index} = \frac{\text{Total Energy} - \text{Absorbed Energy}}{\text{Absorbed Energy}} \quad \text{Eq. 6}$$

As evident from Figure 22 and Figure 23(d), all onyx specimens show high brittle behaviour on comparison with nylon samples. Particularly, it is the Nylon double arrowhead specimen which is found to be most brittle. Nylon Honeycomb, on the other hand, showcased maximum ductility which is also evident from the test sample as no visible defects could be seen through the naked eye.

5.3 Manufacturing Defects and Discrepancies

5.3.1 Mass Defect

Eiger Software was the interface that was used to convert designed CAD files into machine readable codes. After the CAD files were uploaded, and print parameters were assigned, Eiger provided an approximate value of print mass, print volume and the printing time. A discrepancy was found in the components that were printed using the Onyx material in the Eiger software as shown in Table 7.

Table 7 Discrepancy in the theoretical and actual weight

| Core Configuration | Mass (g) ^{Theoretical} * | Mass (g) ^{Actual} | Mass (g) ^{Actual} / Mass (g) ^{Theoretical} |
|--|-----------------------------------|----------------------------|--|
| Out of plane Re-entrant (Nylon) | 28 | 27.7 | 0.989285714 |
| Out of plane Double Arrowhead (Nylon) | 27.7 | 27.55 | 0.994584838 |
| Out of plane Honeycomb (Nylon) | 17.99 | 17.86666667 | 0.993144339 |
| Out of plane Re-entrant (Onyx) | 46.75 | 36.1 | 0.772192513 |
| Out of plane Double Arrowhead (Onyx) | 47 | 36.18 | 0.769787234 |
| Out of plane Honeycomb (Onyx) | 31.33 | 23.82 | 0.760293648 |

*(as per Eiger Software)

The theoretical mass of the specimens was checked using Eiger and actual mass was checked using Kern FKB 8K0.1 weighing scale with a least count of 0.1g. All the Onyx specimens were around 77% of the theoretical mass. This result would vary the density of the Onyx materials which might change the mechanical characteristics of the specimen from the standard specifications. As both Eiger and Onyx is owned by Markforged, the defect needs to be resolved.

5.3.2 Printing Errors

Throughout the project, there were several errors that were faced during the printing process. Repeatability of samples remained one of the key concerns particularly with nylon prints, as nylon prints tended to shrink drastically which led to warping of the specimen about the edges. Another defect during the printing was the dislocation error that occurred on two occasions throughout the project. In this error, the print continued to work without the nylon resin bonding to the print specimen. The following defect can be seen in Figure 24. The following error was rectified by checking the bed levelling.

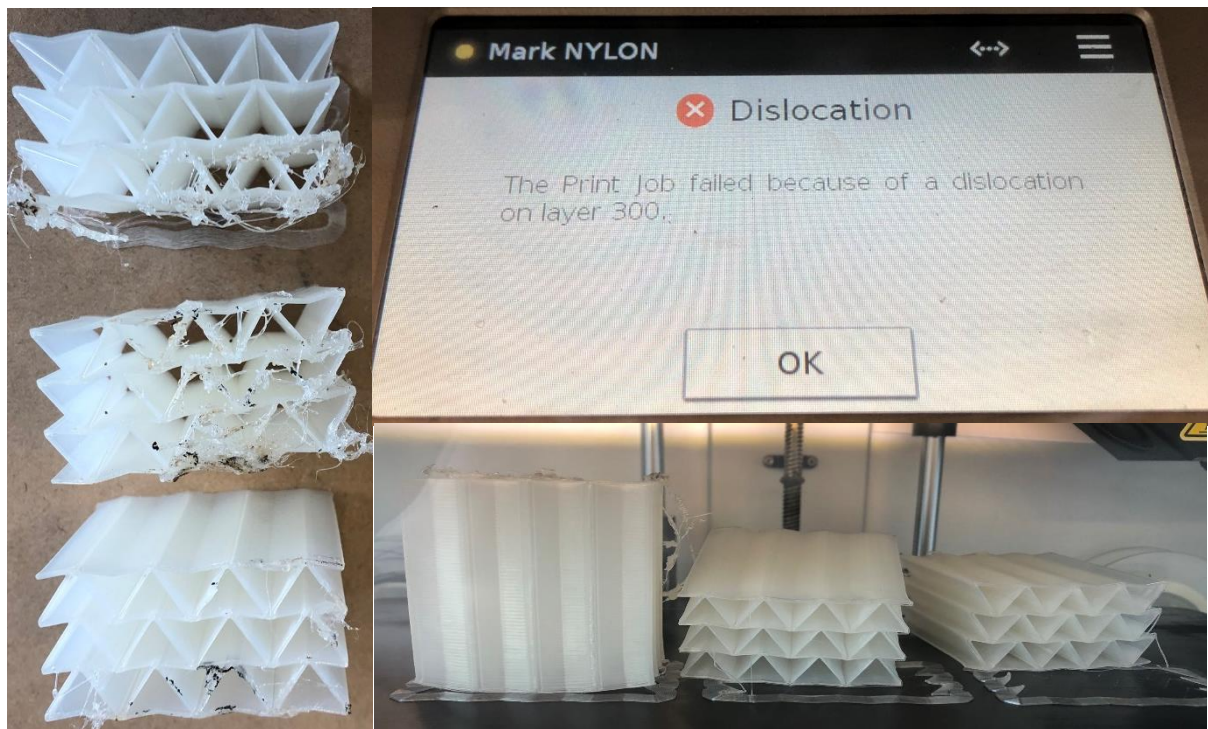


Figure 24. Printing defect caused by a dislocation

The printing of Onyx specimen was more convenient as the material did not contract much on cooling. But while printing an onyx specimen for a different project, Bowden tube was broken off which feeds the filament to the printer. As a result, the complete spool of filament became unusable as a result. The remaining Onyx samples were then manufactured at the NITC facility.

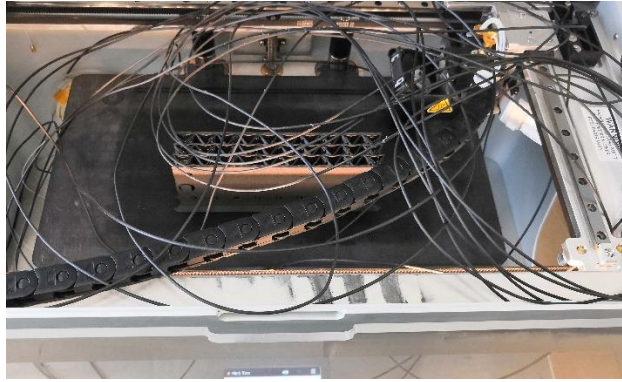


Figure 25. Printing error caused by broken Bowden Tube

6.0 Conclusions

In the following study, the effect of a low velocity impact on auxetic and non-auxetic structures in the form of double arrowhead, re-entrant and honeycomb specimens were studied. The specimens were designed in Solidworks and produced using Markforged Mark Two 3D printers through the process of Fused Deposition Modelling. The specimens were manufactured as per the ASTM d3763 test standard using Nylon and Onyx filament.

It was seen that auxetic structures had better indentation resistance and energy absorption capabilities as compared to non-auxetic structure (honeycomb). However, comparing the double arrowhead and re-entrant structures when subjected to low velocity impact, results were not reliable enough to make a comment. By plotting the Force-Displacement graphs, it was evident that Onyx specimens were brittle in nature, on comparing with Nylon specimens. Even after showcasing better energy absorption characteristics on some parameters, Onyx specimens were punctured through the top layer, penetrating through the structure, which was absent in Nylon. Nylon showcased better mechanical characteristics over Onyx when subjected to indentation impacts, making Nylon more suitable for indentation resistance applications.

6.1 Future Scope

The experiment was carried out on a 30-year-old machine with low calibration and 3 samples per specimen which resulted in ambiguous data. Either the sample size can be increased, or a better calibrated machine can be used to generate reliable data points. A numerical analysis simulating the test parameters can be used to check the accuracy of the data. Additionally, sandwich structures can be produced as a single 3D print and test for indentation tests to compare the effect of indentation on both sandwich structures and core structures.

References

- Aktaş, M., Atas, C., İçten, B. and Karakuzu, R. (2009). An experimental investigation of the impact response of composite laminates. *Composite Structures*, 87(4), pp.307-313.
- Alderson, A. (1999). A triumph of lateral thought Chemistry & Industry, pp.384-391.
- Alderson, A. and Alderson, K. (2007). Auxetic materials. Proceedings of the Institution of Mechanical Engineers, Part G: Journal of Aerospace Engineering, 221(4), pp.565-575.
- Alderson, A., Alderson, K., Chirima, G., Ravirala, N. and Zied, K. (2010). The in-plane linear elastic constants and out-of-plane bending of 3-coordinated ligament and cylinder-ligament honeycombs. *Composites Science and Technology*, 70(7), pp.1034-1041.
- Alderson, A., Rasburn, J., Ameer-Beg, S., Mullarkey, P., Perrie, W. and Evans, K. (2000). An Auxetic Filter: A Tuneable Filter Displaying Enhanced Size Selectivity or Defouling Properties. *Industrial & Engineering Chemistry Research*, 39(3), pp.654-665.
- Alderson, A., Rasburn, J. and Evans, K. (2007). Mass transport properties of auxetic (negative Poisson's ratio) foams. *physica status solidi (b)*, 244(3), pp.817-827.
- Alderson, A., Rasburn, J., Evans, K. and Grima, J. (2001). Auxetic polymeric filters display enhanced de-fouling and pressure compensation properties. *Membrane Technology*, 2001(137), pp.6-8.
- Alderson, K., Alderson, A., Anand, S., Simkins, V., Nazare, S. and Ravirala, N. (2012). Auxetic warp knit textile structures. *physica status solidi (b)*, 249(7), pp.1322-1329.
- Alderson, K., Alderson, A., Ravirala, N., Simkins, V. and Davies, P. (2012). Manufacture and characterisation of thin flat and curved auxetic foam sheets. *physica status solidi (b)*, 249(7), pp.1315-1321.
- Ali, M. and Rehman, I. (2015). Auxetic polyurethane stents and stent-grafts for the palliative treatment of squamous cell carcinomas of the proximal and mid oesophagus: A novel fabrication route. *Journal of Manufacturing Systems*, 37, pp.375-395.
- Alomarah, A., Zhang, J., Ruan, D., Masood, S. and Lu, G. (2017). Mechanical Properties of the 2D Re-entrant Honeycomb Made via Direct Metal Printing. *IOP Conference Series: Materials Science and Engineering*, 229, p.012038.
- Álvarez Elípe, J. and Díaz Lantada, A. (2012). Comparative study of auxetic geometries by means of computer-aided design and engineering. *Smart Materials and Structures*, 21(10), p.105004.
- Andrews, E., Gibson, L. and Ashby, M. (1999). The creep of cellular solids. *Acta Materialia*, 47(10), pp.2853-2863.
- Argatov, I., Guinovart-Díaz, R. and Sabina, F. (2012). On local indentation and impact compliance of isotropic auxetic materials from the continuum mechanics viewpoint. *International Journal of Engineering Science*, 54, pp.42-57.
- ASTM D3763-10, Standard Test Method for High Speed Puncture Properties of Plastics Using Load and Displacement Sensors, ASTM International, West Conshohocken, PA, 2010, www.astm.org
- Attard, D. and Grima, J. (2008). Auxetic behaviour from rotating rhombi. *physica status solidi (b)*, 245(11), pp.2395-2404.

Belingardi, G. and Vadori, R. (2002). Low velocity impact tests of laminate glass-fiber-epoxy matrix composite material plates. *International Journal of Impact Engineering*, 27(2), pp.213-229.

Bratfisch, J. and Vandepitte, D. (2007). Development and Validation of a Continuous Production Concept for Thermoplastic Honeycomb. *Journal of Sandwich Structures & Materials*, 9(2), pp.113-122.

Choi, J. and Lakes, R. (1991). Design of a fastener based on negative Poisson's ratio foam. *Cellular Polymers*, 10, pp.205-212.

Choi, J. and Lakes, R. (1996). Fracture toughness of re-entrant foam materials with a negative Poisson's ratio: experiment and analysis. *International Journal of Fracture*, 80(1), pp.73-83.

Choi, J. and Lakes, R. (1992). Non-linear properties of metallic cellular materials with a negative Poisson's ratio. *Journal of Materials Science*, 27(19), pp.5375-5381.

Christensen, J., Kadic, M., Kraft, O. and Wegener, M. (2015). Vibrant times for mechanical metamaterials. *MRS Communications*, 5(03), pp.453-462.

Critchley, R., Corni, I., Wharton, J., Walsh, F., Wood, R. and Stokes, K. (2013). A review of the manufacture, mechanical properties and potential applications of auxetic foams. *physica status solidi (b)*, p.n/a-n/a.

Dikshit, V., Yap, Y., Goh, G., Yang, H., Lim, J., Qi, X., Yeong, W. and Wei, J. (2016). Investigation of out of plane compressive strength of 3D printed sandwich composites. *IOP Conference Series: Materials Science and Engineering*, 139, p.012017.

Evans, K. and Alderson, A. (2000). Auxetic Materials: Functional Materials and Structures from Lateral Thinking!. *Advanced Materials*, 12(9), pp.617-628.

Fan, X., Verpoest, I., Pflug, J., Vandepitte, D. and Bratfisch, P. (2009). Investigation of Continuously Produced Thermoplastic Honeycomb Processing — Part I: Thermoforming. *Journal of Sandwich Structures & Materials*, 11(2-3), pp.151-178.

Ferguson, W., Kuang, Y., Evans, K., Smith, C. and Zhu, M. (2018). Auxetic structure for increased power output of strain vibration energy harvester. *Sensors and Actuators A: Physical*, 282, pp.90-96.

Fu, M., Xu, O., Hu, L. and Yu, T. (2016). Nonlinear shear modulus of re-entrant hexagonal honeycombs under large deformation. *International Journal of Solids and Structures*, 80, pp.284-296.

Gatt, R., Attard, D., Farrugia, P., Azzopardi, K., Mizzi, L., Brincat, J. and Grima, J. (2013). A realistic generic model for anti-tetrachiral systems. *physica status solidi (b)*, p.n/a-n/a.

Gao, Q., Ge, C., Zhuang, W., Wang, L. and Ma, Z. (2019). Crashworthiness analysis of double-arrowed auxetic structure under axial impact loading. *Materials & Design*, 161, pp.22-34.

Gibson, L., Ashby, M., Schajer, G. and Robertson, C. (1982). The Mechanics of Two-Dimensional Cellular Materials. *Proceedings of the Royal Society A: Mathematical, Physical and Engineering Sciences*, 382(1782), pp.25-42.

Grima, J., Caruana-Gauci, R., Dudek, M., Wojciechowski, K. and Gatt, R. (2013). Smart metamaterials with tunable auxetic and other properties. *Smart Materials and Structures*, 22(8), p.084016.

Grima, J. and Evans, K. (2006). Auxetic behavior from rotating triangles. *Journal of Materials Science*, 41(10), pp.3193-3196.

Grima, J., Farrugia, P., Caruana, C., Gatt, R. and Attard, D. (2008). Auxetic behaviour from stretching connected squares. *Journal of Materials Science*, 43(17), pp.5962-5971.

Grima, J., Oliveri, L., Attard, D., Ellul, B., Gatt, R., Cicala, G. and Recca, G. (2010). Hexagonal Honeycombs with Zero Poisson's Ratios and Enhanced Stiffness. *Advanced Engineering Materials*, 12(9), pp.855-862.

Grima, J., Winczewski, S., Mizzi, L., Grech, M., Cauchi, R., Gatt, R., Attard, D., Wojciechowski, K. and Rybicki, J. (2014). Tailoring Graphene to Achieve Negative Poisson's Ratio Properties. *Advanced Materials*, 27(8), pp.1455-1459.

Hall, L., Coluci, V., Galvao, D., Kozlov, M., Zhang, M., Dantas, S. and Baughman, R. (2008). Sign Change of Poisson's Ratio for Carbon Nanotube Sheets. *Science*, 320(5875), pp.504-507.

Harkati, E., Daoudi, N., Bezazi, A., Haddad, A. and Scarpa, F. (2017). In-plane elasticity of a multi re-entrant auxetic honeycomb. *Composite Structures*, 180, pp.130-139.

Hou, S., Li, T., Jia, Z. and Wang, L. (2018). Mechanical properties of sandwich composites with 3d-printed auxetic and non-auxetic lattice cores under low velocity impact. *Materials & Design*, 160, pp.1305-1321.

Imbalzano, G., Linforth, S., Ngo, T., Lee, P. and Tran, P. (2018). Blast resistance of auxetic and honeycomb sandwich panels: Comparisons and parametric designs. *Composite Structures*, 183, pp.242-261.

Imbalzano, G., Tran, P., Ngo, T. and Lee, P. (2016). A numerical study of auxetic composite panels under blast loadings. *Composite Structures*, 135, pp.339-352.

Jin, X., Hou, C., Fan, X., Sun, Y., Lv, J. and Lu, C. (2018). Investigation on the static and dynamic behaviors of non-pneumatic tires with honeycomb spokes. *Composite Structures*, 187, pp.27-35.

Lakes, R. and Elms, K. (1993). Indentability of Conventional and Negative Poisson's Ratio Foams. *Journal of Composite Materials*, 27(12), pp.1193-1202.

Larsen, U., Signund, O. and Bouwsta, S. (1997). Design and fabrication of compliant micromechanisms and structures with negative Poisson's ratio. *Journal of Microelectromechanical Systems*, 6(2), pp.99-106.

Li, T. and Wang, L. (2017). Bending behavior of sandwich composite structures with tunable 3D-printed core materials. *Composite Structures*, 175, pp.46-57.

Li, X., Lu, Z., Yang, Z. and Yang, C. (2017). Directions dependence of the elastic properties of a 3D augmented re-entrant cellular structure. *Materials & Design*, 134, pp.151-162.

Lorato, A., Innocenti, P., Scarpa, F., Alderson, A., Alderson, K., Zied, K., Ravirala, N., Miller, W., Smith, C. and Evans, K. (2010). The transverse elastic properties of chiral honeycombs. *Composites Science and Technology*, 70(7), pp.1057-1063.

Masters, I. and Evans, K. (1996). Models for the elastic deformation of honeycombs. *Composite Structures*, 35(4), pp.403-422.

- Mohsenizadeh, S., Alipour, R., Shokri Rad, M., Farokhi Nejad, A. and Ahmad, Z. (2015). Crashworthiness assessment of auxetic foam-filled tube under quasi-static axial loading. *Materials & Design*, 88, pp.258-268.
- Novak, N., Vesenjaj, M. and Ren, Z. (2016). Auxetic Cellular Materials - a Review. *Strojniški vestnik – Journal of Mechanical Engineering*, 62(9), pp.485-493.
- Panowicz, R. and Miedzińska, D. (2012). Numerical and experimental research on polyisocyanurate foam. *Computational Materials Science*, 64, pp.126-129.
- Prall, D. and Lakes, R. (1997). Properties of a chiral honeycomb with a poisson's ratio of — 1. *International Journal of Mechanical Sciences*, 39(3), pp.305-314.
- Prawoto, Y. (2012). Seeing auxetic materials from the mechanics point of view: A structural review on the negative Poisson's ratio. *Computational Materials Science*, 58, pp.140-153.
- Qiao, J. and Chen, C. (2015). Impact resistance of uniform and functionally graded auxetic double arrowhead honeycombs. *International Journal of Impact Engineering*, 83, pp.47-58.
- Rafsanjani, A. and Pasini, D. (2016). Bistable auxetic mechanical metamaterials inspired by ancient geometric motifs. *Extreme Mechanics Letters*, 9, pp.291-296.
- Raghunath, G., Flatau, A., Wang, H. and Wu, R. (2016). Magnetoelastic auxetic-like behavior in Galfenol: Experimental data and simulations. *physica status solidi (b)*, 253(7), pp.1440-1448.
- Ren, X., Das, R., Tran, P., Ngo, T. and Xie, Y. (2018). Auxetic metamaterials and structures: a review. *Smart Materials and Structures*, 27(2), p.023001.
- Ren, X., Shen, J., Tran, P., Ngo, T. and Xie, Y. (2018). Auxetic nail: Design and experimental study. *Composite Structures*, 184, pp.288-298.
- Sanami, M., Ravirala, N., Alderson, K. and Alderson, A. (2014). Auxetic Materials for Sports Applications. *Procedia Engineering*, 72, pp.453-458.
- Saxena, K., Das, R. and Calius, E. (2016). Three Decades of Auxetics Research – Materials with Negative Poisson's Ratio: A Review. *Advanced Engineering Materials*, 18(11), pp.1847-1870.
- Scarpa, F., Adhikari, S. and Srikantha Phani, A. (2009). Effective elastic mechanical properties of single layer graphene sheets. *Nanotechnology*, 20(6), p.065709.
- Schaedler, T. and Carter, W. (2016). Architected Cellular Materials. *Annual Review of Materials Research*, 46(1), pp.187-210.
- Schwerdtfeger, J., Heinl, P., Singer, R. and Körner, C. (2010). Auxetic cellular structures through selective electron-beam melting. *physica status solidi (b)*, 247(2), pp.269-272.
- Shivakumar, K., Elber, W. and Illg, W. (1985). Prediction of low-velocity impact damage in thin circular laminates. *AIAA Journal*, 23(3), pp.442-449.
- Shokri Rad, M., Ahmad, Z. and Alias, A. (2015). Computational Approach in Formulating Mechanical Characteristics of 3D Star Honeycomb Auxetic Structure. *Advances in Materials Science and Engineering*, 2015, pp.1-11.
- Simkins, V., Alderson, A., Davies, P. and Alderson, K. (2005). Single fibre pullout tests on auxetic polymeric fibres. *Journal of Materials Science*, 40(16), pp.4355-4364.
- Sivák, P., Delyová, I. and Diabelková, P. (2017). Analysis of Sandwich Structures by the FEM. *American Journal of Mechanical Engineering*, Vol. 5, No. 6, pp 243-246.

Tretiakov, K. and Wojciechowski, K. (2012). Elasticity of two-dimensional crystals of polydisperse hard disks near close packing: Surprising behavior of the Poisson's ratio. *The Journal of Chemical Physics*, 136(20), p.204506.

Wang, Y. and Lakes, R. (2002). Analytical parametric analysis of the contact problem of human buttocks and negative Poisson's ratio foam cushions. *International Journal of Solids and Structures*, 39(18), pp.4825-4838.

Wang, Y., Wang, L., Ma, Z. and Wang, T. (2016). A negative Poisson's ratio suspension jounce bumper. *Materials & Design*, 103, pp.90-99.

Wang, Y., Zhao, W., Zhou, G. and Wang, C. (2018). Analysis and parametric optimization of a novel sandwich panel with double-V auxetic structure core under air blast loading. *International Journal of Mechanical Sciences*, 142-143, pp.245-254.

Wang, Z. (2019). Recent advances in novel metallic honeycomb structure. *Composites Part B: Engineering*, 166, pp.731-741.

Wollner, U., Vanorio, T. and Kiss, A. (2018). The effect of fluid and solid properties on the auxetic behavior of porous materials having rock-like microstructures. *International Journal of Solids and Structures*, 130-131, pp.211-219.

Xu, Y., Uddin, S., Wang, J., Wu, J. and Liu, J. (2017). Penetration depth and nonlocal manipulation of quantum spin hall edge states in chiral honeycomb nanoribbons. *Scientific Reports*, 7(1).

Yang, L., Harrysson, O., Cormier, D., West, H., Gong, H. and Stucker, B. (2015). Additive Manufacturing of Metal Cellular Structures: Design and Fabrication. *JOM*, 67(3), pp.608-615.

Yang, L., Harrysson, O., West, H. and Cormier, D. (2015). Mechanical properties of 3D re-entrant honeycomb auxetic structures realized via additive manufacturing. *International Journal of Solids and Structures*, 69-70, pp.475-490.

Yang, S., Qi, C., Wang, D., Gao, R., Hu, H. and Shu, J. (2013). A Comparative Study of Ballistic Resistance of Sandwich Panels with Aluminum Foam and Auxetic Honeycomb Cores. *Advances in Mechanical Engineering*, 5, p.589216.

Yap, Y. and Yeong, W. (2015). Shape recovery effect of 3D printed polymeric honeycomb. *Virtual and Physical Prototyping*, 10(2), pp.91-99.

Yazdani Sarvestani, H., Akbarzadeh, A., Niknam, H. and Hermenean, K. (2018). 3D printed architected polymeric sandwich panels: Energy absorption and structural performance. *Composite Structures*, 200, pp.886-909.

Zeng, J., Hu, H. and Zhou, L. (2017). A study on negative Poisson's ratio effect of 3D auxetic orthogonal textile composites under compression. *Smart Materials and Structures*, 26(6), p.065014.

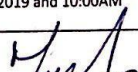
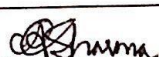
Zhou, G., Ma, Z., Li, G., Cheng, A., Duan, L. and Zhao, W. (2016). Design optimization of a novel NPR crash box based on multi-objective genetic algorithm. *Structural and Multidisciplinary Optimization*, 54(3), pp.673-684.

Appendix A Project management



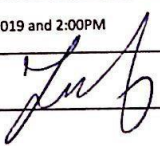
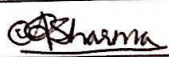
**SCHOOL OF
MECHANICAL
AND AEROSPACE
ENGINEERING**

Individual Project Meeting Record

| | | | |
|--|---|--------------------------|---|
| Project Title | Low-velocity impact analysis of auxetic cored sandwich panels | | |
| Supervisor | Dr. Zafer Kazanci | Student | Aayush Sharma |
| Date and time | 28/05/2019 and 12:30PM | Location | ASH 06.014 |
| <p>Review of actions from previous meeting No Previous Meeting</p> | | | |
| <p>Discussion, decisions, assignments Introduction to Auxetic Structures, their types based on material (PU Foams) and shape (re-entrant honeycomb, double arrow-head etc.). Auxetic Structures showcase high impact resistance compared to non-auxetic structures with similar parameters. The aim of the project is to find the gaps in presented literature and try to fill some of those gaps to get a relevant and impacting result.</p> | | | |
| <p>Agreed actions and completion dates Reading 4-5 review articles on Auxetic Sandwich Panels. Meeting with Clare Burnett (PhD Student) to discuss the project.</p> | | | |
| Date and time of next meeting | 13/06/2019 and 10:00AM | Location of next meeting | ASH 06.014 |
| Supervisor signature |  | Student signature |  |

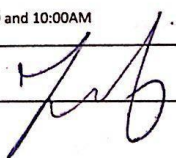
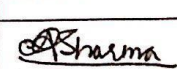


Individual Project Meeting Record

| | | | |
|--|---|--------------------------|---|
| Project Title | Low-velocity impact analysis of auxetic cored sandwich panels | | |
| Supervisor | Dr. Zafer Kazanci | Student | Aayush Sharma |
| Date and time | 13/06/2019 and 10:00AM | Location | ASH 06.014 |
| <p>Review of actions from previous meeting Literature Review on auxetic structures was checked by Dr Kazanci. More literature focussed on Auxetic sandwich panels was required.</p> <p>Discussion, decisions, assignments Risk assessment form as a prerequisite to work on the project was reviewed by Dr Kazanci. Reports of 2 former students working on Auxetic materials was provided to get broader context on the topic. Using Numerical Modelling technique to theorise the experiment and performing the experiment practically and comparing the results to check the relevance of data provided.</p> <p>Agreed actions and completion dates To complete a numerical analysis of an auxetic sandwich panel subjected to low velocity impact. To complete the Health and Safety Lab Induction.</p> | | | |
| Date and time of next meeting | 26/06/2019 and 2:00PM | Location of next meeting | ASH 06.014 |
| Supervisor signature |  | Student signature |  |

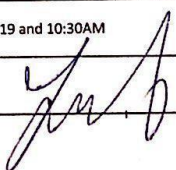
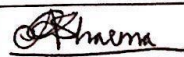


Individual Project Meeting Record

| | | | |
|---|---|--------------------------|---|
| Project Title | Low-velocity impact analysis of auxetic cored sandwich panels | | |
| Supervisor | Dr. Zafer Kazanci | Student | Aayush Sharma |
| Date and time | 26/06/2019 and 2:00PM | Location | ASH 06.014 |
| <p>Review of actions from previous meeting The numerical modelling on low-velocity impact test on auxetic sandwich panels was still under way.</p> <p>Completion of Health and Safety Lab Induction.</p> <p>Discussion, decisions, assignments An idea to 3D print the complete sandwich panel as a single body with auxetic core and cover facesheets of the same material was presented that would save the assembly time and reduce bonding defects.</p> <p>Metal facesheets have a drawback that they absorb low-velocity impact and no considerable change in the core can be seen, producing no significant results.</p> <p>Agreed actions and completion dates To prepare a clear and concise testing plan.</p> <p>To present the different parameters to work on during the project as potential gaps in the literature.</p> <p>To order some material for testing purposes.</p> <p>To check the working of Mark Forged 3D printer from the demonstration.</p> | | | |
| Date and time of next meeting | 04/07/2019 and 10:00AM | Location of next meeting | ASH 06.014 |
| Supervisor signature |  | Student signature |  |

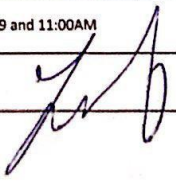
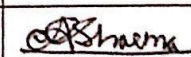


Individual Project Meeting Record

| | | | |
|---|---|--------------------------|---|
| Project Title | Low-velocity impact analysis of auxetic cored sandwich panels | | |
| Supervisor | Dr. Zafer Kazanci | Student | Aayush Sharma |
| Date and time | 04/07/2019 and 10:00AM | Location | ASH 06.014 |
| <p>Review of actions from previous meeting A spool of Markforged Nylon Filament 800cm³ was ordered. The working of Markforged 3D printers was demonstrated by Clare Burnett while printing a double arrowhead auxetic core.</p> <p>Discussion, decisions, assignments Found a gap in literature and discussed about finding a possible relation between the low velocity impact of an auxetic sandwich structure on its relative density by changing one of the internal angles of the auxetic lattice structure. Double arrowhead and re-entrant hexagonal lattices were chosen for the experiment as these structures provided with highest impact resistance as per the literature.</p> <p>Agreed actions and completion dates Completion of the project plan with auxetic structure designs ready to print.</p> | | | |
| Date and time of next meeting | 23/07/2019 and 10:30AM | Location of next meeting | ASH 06.014 |
| Supervisor signature |  | Student signature |  |

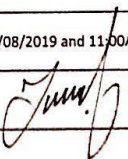


Individual Project Meeting Record

| | | | |
|---|---|--------------------------|---|
| Project Title | Low-velocity impact analysis of auxetic cored sandwich panels | | |
| Supervisor | Dr. Zafer Kazanci | Student | Aayush Sharma |
| Date and time | 23/07/2019 and 10:30AM | Location | ASH 06.014 |
| <p>Review of actions from previous meeting The auxetic cored sandwich structures were designed and ready to print. A theoretical calculation was carried out to find the relative density and poisson's ratio of the designed sandwich structures.</p> <p>Discussion, decisions, assignments Importance of Project Plan and written objectives over verbal conversations.</p> <p>Agreed actions and completion dates A brief presentation to provide the updates on the project.</p> | | | |
| Date and time of next meeting | 25/07/2019 and 11:00AM | Location of next meeting | ASH 06.014 |
| Supervisor signature |  | Student signature |  |



Individual Project Meeting Record

| | | | |
|--|---|--------------------------|---------------|
| Project Title | Low-velocity impact analysis of auxetic cored sandwich panels | | |
| Supervisor | Dr. Zafer Kazanci | Student | Aayush Sharma |
| Date and time | 25/07/2019 and 11:00AM | Location | ASH 06.014 |
| <p><u>Review of actions from previous meeting</u> A brief presentation to provide the updates on the project.</p> <p><u>Discussion, decisions, assignments</u> Reviewed the presentation about the status of the project. Discussed about using possible impact testing machines available in QUB. To find out a new test standard as per the impact facility available in QUB.</p> <p><u>Agreed actions and completion dates</u> Completion of the numerical analysis and check if 50J energy is required to see some results. Check low velocity energy levels. To try finding out low velocity impact testing machines in QUB facility. To start with printing of cored structures. To prepare a Test Matrix.</p> | | | |
| Date and time of next meeting | 06/08/2019 and 11:00AM | Location of next meeting | ASH 06.014 |
| Supervisor signature |  | Student signature | |

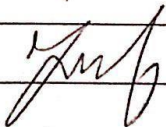


Individual Project Meeting Record

| | | | |
|--|---|--------------------------|---------------|
| Project Title | Low-velocity impact analysis of auxetic cored sandwich panels | | |
| Supervisor | Dr. Zafer Kazanci | Student | Aayush Sharma |
| Date and time | 06/08/2019 and 11:00AM | Location | ASH 06.014 |
| <p>Review of actions from previous meeting Prepared a Test Matrix CEAST Drop Impact Test suitable for low velocity impact test Impact with velocities lower than 10m/s considered as Low velocity Impact Initiated 3D printing of auxetic cores</p> <p>Discussion, decisions, assignments Reduce the number of specimens from 10 to 3 per sample due to less time at hand.</p> <p>Agreed actions and completion dates Completion of printing of auxetic cores. Completion of Drop Impact testing on auxetic cores. Completion of Numerical Analysis of drop impact tests. (Not completed) Completion of a Draft Report. (Not Completed)</p> | | | |
| Date and time of next meeting | 20/08/2019 and 04:00PM | Location of next meeting | ASH 06.014 |
| Supervisor signature | Student signature | | |



Individual Project Meeting Record

| | | | |
|--|---|--------------------------|---------------|
| Project Title | Low-velocity impact analysis of auxetic cored sandwich panels | | |
| Supervisor | Dr. Zafer Kazanci | Student | Aayush Sharma |
| Date and time | 20/08/2019 and 04:00PM | Location | ASH 06.014 |
| <p><u>Review of actions from previous meeting</u> Completion of printing of auxetic cores. Completion of Drop Impact testing on auxetic cores. Working on Numerical Analysis and Draft Report.</p> <p><u>Discussion, decisions, assignments</u></p> <p><u>Agreed actions and completion dates</u> Completion and Submission of Final Report by 24/08/19.</p> | | | |
| Date and time of next meeting | | Location of next meeting | |
| Supervisor signature |  | Student signature | |

Project Submission Checklist

A copy of the checklist can be found on the Student SharePoint site and must be included at the very end of your report.

| | TICK IF MET |
|--|-------------|
| Does the report meet the formatting stipulated in the module handbook and template provided? | ✓ |
| Line spacing (1.5). | ✓ |
| Font (Calibri 11 Pt). | ✓ |
| Margins: Top & Bottom (25 mm), Left (25 mm), Right (25 mm). | ✓ |
| Paragraphs are fully justified. | ✓ |
| Does the main body of the report meet the strict 30 page limit (40 page limit for AER4002 and MEE7012)? (excluding Title Page, Table of Contents, References and Submission Checklist) | ✓ |
| Do the appendices meet the strict 10 page limit (15 page limit for AER4002 and MEE7012)? | ✓ |
| Are all tables and figures numbered correctly, captioned and referenced if required? | ✓ |
| Pages are numbered. | ✓ |
| Has the project description (as submitted in Week 8, with any subsequent changes agreed with your supervisor) been included in the report? | ✓ |

Statement of originality

I hereby declare that this project is my own work and that it has not been submitted for another degree, either at Queen's University Belfast or elsewhere. Where other sources of information have been used, they have been acknowledged.

Signature: *Shayna*

Date: 30th August '19